

#### **OPEN ACCESS**

EDITED BY

Surendra Pratap Singh, Chhatrapati Shahu Ji Maharaj University, India

REVIEWED BY

Gildemberg Amorim Leal Junior, Federal University of Alagoas, Brazil Feihong Liang, The Northwest Institute of Eco-Environment and Resources, China

\*CORRESPONDENCE

Bin Wang

Mappywangbin2003@163.com

RECEIVED 11 June 2025
ACCEPTED 27 October 2025
PUBLISHED 14 November 2025

#### CITATION

Wang B, Li M, Chen J and Chen L (2025) Genome-wide comprehensive analysis the molecular phylogenetic evolution, functional divergence and tissue-specific expression of *GH3* gene family in *Salvia miltiorrhiza*, *Arabidopsis thaliana*, and Oryza sativa. *Front. Plant Sci.* 16:1644853. doi: 10.3389/fpls.2025.1644853

#### COPYRIGHT

© 2025 Wang, Li, Chen and Chen. This is an open-access article distributed under the terms of the Creative Commons Attribution License (CC BY). The use, distribution or reproduction in other forums is permitted, provided the original author(s) and the copyright owner(s) are credited and that the original publication in this journal is cited, in accordance with accepted academic practice. No use, distribution or reproduction is permitted which does not comply with these terms.

Genome-wide comprehensive analysis the molecular phylogenetic evolution, functional divergence and tissue-specific expression of *GH3* gene family in *Salvia miltiorrhiza*, *Arabidopsis thaliana*, and Oryza sativa

Bin Wang<sup>1,2\*</sup>, Min Li<sup>2,3</sup>, Jun Chen<sup>2</sup> and Longtao Chen<sup>2</sup>

<sup>1</sup>College of Life Sciences, Henan Normal University, Xinxiang, China, <sup>2</sup>School of Science, East China University of Technology, Nanchang, China, <sup>3</sup>Life Science & Technology School, Lingnan Normal University, Zhanjiang, China

Auxin, as a central phytohormone and signaling molecule, plays a crucial role in plant growth and development. The activity of auxin is tightly regulated by the auxin-responsive GH3 gene family. In this study, a total of 40 GH3 genes in A. thaliana, S. miltiorrhiza, and O. sativa were identified and subjected to comprehensive study. Phylogenetic analysis revealed that those GH3 genes can be classified into three distinct subgroups, with 11 pairs of paralogs identified. Genetic divergence analysis indicated that the GH3 gene family had predominantly experienced purifying selection as evidenced by the Ka/Ks ratio being less than 1 for all 11 paralogs pairs. Positive selection analysis with the site and branch-site models further suggested that SmGH3 AtGH3 and OsGH3 genes had gone through purifying selective pressure for adaptive evolution. Motif analysis indicated that group-specific motifs may contribute to functional divergence across species and subgroups. Functional divergence analysis confirmed that subgroup-specific genes have experienced functional divergence during evolution, and elucidated the molecular mechanisms underlying their divergent functions. The tissue-specific expression analysis of SmGH3 AtGH3 and OsGH3 genes revealed that these genes might perform distinct functions in different tissues. This study performed a comprehensive bioinformatics analysis of the GH3 gene family, offering valuable information to further elucidate the functional roles of GH3 genes.

#### KEYWORDS

conserved motifs, functional divergence, GH3 gene family, nonsynonymous and synonymous substitution rate, phylogenetic analysis, positive selection, tissue-specific expression

## 1 Introduction

Auxin plays a crucial role in regulating various aspects of plant development and growth, such as apical dominance, auxin transport, shoot elongation, and plant metabolism (Woodward and Bartel, 2005; Baranwal et al., 2017). A wide array of these processes are modulated by auxin-responsive genes, primarily including Auxin Response Factor (ARF) genes, which function as transcriptional activators, Small Auxin Up RNA (SAUR) genes, which regulate auxin signaling pathways, Auxin/Indole-3-Acetic Acid (AUX/IAA) genes, which act as transcriptional repressors, and Gretchen Hagen 3 (GH3) genes, which regulate the dynamic process of endogenous auxin homeostasis (Hagen and Guilfoyle, 1984; Fu et al., 2011; Chen et al., 2014; Kong et al., 2019). Moreover, GH3-mediated auxin regulation constitutes an essential component of the intricate network of auxin activity that governs plant responses to environmental stresses (Wang et al., 2010). Thus, the GH3 gene family primarily comprises a series of genes that encode specific enzymes, which capable of conjugating various amino acids to chemically diverse compounds (Kong et al., 2019). Typically, the GH3 gene family is significantly influenced by various hormones, including growth-promoting hormones such as brassinosteroids (BRs) and gibberellins (GA), stress-related hormones like abscisic acid (ABA), jasmonic acid (JA), and salicylic acid (SA), as well as the ripening/senescence-associated hormone Ethylene (ETH). Besides, these genes are responsive to biotic stresses caused by pathogens and abiotic stress factors such as light, salt, drought, cold, and other environmental stresses (Shin-Ichiro et al., 2002; Park et al., 2007; Zhang et al., 2009; Takase et al., 2010; Wang et al., 2010).

The first GH3 gene was identified in soybean (Glycine max) through differential hybridization analysis, where it was found to be responsive to the plant hormone auxin (Hagen and Guilfoyle, 1984). Since then, GH3 genes have been reported in various plant species (Terol et al., 2006; Okrent and Wildermuth, 2011). The GH3 gene family was first characterized in the model organism Arabidopsis thaliana (A. thaliana), with 19 distinct members identified (Staswick et al., 2002). Through genome-wide analysis, an increasing number of GH3 genes family have been successively identified in diverse species, including 13 in Oryza sativa (O. sativa) (Jain et al., 2006a), 9 in grape (Bottcher et al., 2011), 13 in maize (Feng et al., 2015), 15 in rosids (Okrent and Wildermuth, 2011), 15 in tomato (Kumar et al., 2012), and in legumes (11 in chickpea, 28 in soybean, 10 in Medicago, and 18 in Lotus) (Singh et al., 2014), 15 in apple (Yuan et al., 2013), and 10 in Melon (Chen et al., 2023). The number of GH3 genes varies across different plant species and is closely associated with the expansion and diversification of the gene family. However, the evolutionary dynamics and molecular mechanisms underlying the diversification of the GH3 gene family remain poorly understood. Elucidating these mechanisms is essential for understanding the roles of GH3 genes in plant evolution and adaptation.

Based on the sequence similarity and substrate specificity analyses, GH3 proteins are typically classified into three distinct clades (I, II, and III) using distance-based phylogenetic methods (Staswick et al., 2002, 2005; Okrent et al., 2009). Proteins in clade I primarily exhibit JA- or SA-amido synthetase activity, using JA or SA as substrates to synthesize corresponding amide conjugates such as JA-Ile or SA-amide compounds (Staswick et al., 2002). Proteins from clade II are responsive to auxin and exhibit auxin-inducible expression profiles (Staswick et al., 2005). The functions of most clade III GH3 proteins remain not yet fully characterized (Kong et al., 2019), although certain clade III proteins have been found to be induced in response to infection by *Pseudomonas syringae* (Nobuta et al., 2007; Okrent et al., 2009). The functional divergence observed during the phylogenetic evolution of *GH3* genes is notable, and this functional specialization undoubtedly underscores the complexity of the molecular mechanism involved. However, the molecular mechanisms underlying these functional divergences remain unexplored and require further investigation.

S. miltiorrhiza a well-known member of traditional Chinese medicine, is widely utilized for treating various cerebrovascular and cardiovascular disorders (Zhou et al., 2005; Geng et al., 2015). The pharmacological activities of S. miltiorrhiza can be attributed to its two primary bioactive components. One group consists of lipidsoluble diterpenoids, commonly referred to as tanshinones, while the other comprises water-soluble phenolic acids, such as rosmarinic acid (RA) and salvianolic acid B (Sal B) (Ma et al., 2012; Wang et al., 2018). The biosynthetic pathways responsible for the production of these two pharmacologically active components in S. miltiorrhiza are modulated by various plant hormone signals, including SA, JA, IAA and ABA, which collectively influence the synthesis and accumulation of its medicinal constituents (Zhao et al., 2010; Cui et al., 2012; Ge et al., 2015; Huang et al., 2023). Additionally, members of the GH3 protein family play a crucial role in maintaining auxin homeostasis through enzymatic catalysis of amino acid conjugation to phytohormones such as IAA, SA, and JA (Staswick et al., 2002, 2005). These enzymatic reaction processes and their products may be associated with the regulation of hormone signaling pathways and secondary metabolism in S. miltiorrhiza. Due to its relatively small genome and wellcharacterized secondary metabolic pathways, S. miltiorrhiza is recommended by many researchers as a model medicinal plant in the field of medicinal plant research (Ma et al., 2012; Xu et al., 2015). Likewise, A. thaliana is widely recognized as a model organism in plant research due to its small genome size and short growth cycle. Similarly, O. sativa has been established as a genetic, molecular, and functional model organism for research due to its importance as a major food crop (Yang et al., 2008). The objective of our study is to perform a comprehensive phylogenomic analysis of the GH3 gene family across three plant species, with the aim of elucidating the molecular evolution mechanisms underlying their evolutionary dynamics, genetic and functional divergence of this gene family during their evolution.

Recent advancements in high-throughput sequencing technologies have significantly expanded access to plant genome and transcriptome databases, providing robust analytical platforms for studying gene expression and functional characterization. Expressed sequence tags (ESTs), short cDNA fragments derived from various tissues, represent partial sequences of transcribed

genes and provide valuable tools for analyzing mRNA expression profiles (Ohlrogge and Benning, 2000). Thus, the relative frequency of ESTs or full-length cDNAs across different databases serves as an efficient tool for preliminary analysis of gene expression patterns in different tissues (Adams et al., 1995). Therefore, the transcriptomes of different tissues from *S. miltiorrhiza* (Zhang et al., 2015) and the GenBank EST databases (https://www.ncbi.nlm.nih.gov/genbank/dbest/) (Boguski et al., 1993) for *A. thaliana* and *O. sativa* collectively provide comprehensive insights into genetic transcription, thereby enabling more systematic and detailed analyses of *GH3* gene expression across these species.

In this study, following the identification of the GH3 gene family in S. miltiorrhiza, we conducted a comprehensive bioinformatics analysis of the GH3 gene families across A. thaliana, S. miltiorrhiza, and O. sativa. We first examined the conserved domains, gene structure, motifs and cis-regulatory elements of those genes. Subsequently, we constructed a phylogenetic tree to evaluate the evolutionary relationships among the SmGH3, AtGH3, and OsGH3 genes. To investigate the selective pressures driving gene divergence, we calculated the Ka/Ks ratios for paralogous gene pairs. Using site and branch-site models, we detected positive selection in the SmGH3, AtGH3, and OsGH3 genes with the PAML program. Additionally, we analyzed functional divergence among the SmGH3, AtGH3, and OsGH3 genes using the DIVERGE program. Finally, the tissue-specific expression patterns of the SmGH3, AtGH3, and OsGH3 genes were preliminarily evaluated using the EST database and RNAseq data.

### 2 Methods

## 2.1 Identification of the members of *GH3* in *S. miltiorrhiza, A. thaliana,* and *O. sativa*

Using the TAIR (The Arabidopsis Information Resource) database (Garcia-Hernandez et al., 2002) and RAP (Rice Annotation Project) database (Sakai et al., 2013), we obtained the amino acids sequences of 19 AtGH3 and 13 OsGH3, respectively. Then, employing the BioEdit software (Hall, 1999), we used these amino acid sequences as queries to search the current S. miltiorrhiza genome assembly, which covers approximately 92% of the entire genome and 96% of the protein-coding genes (Song et al., 2013; Xu et al., 2016) under the BLASTp program (Altschul et al., 1997). Finally, following the previously established methods for screening gene family members (Wang et al., 2017, 2019) and the basic characteristics of GH3 protein, we identified the GH3 gene family in S. miltiorrhiza. The theoretical isoelectric point (pI) and molecular weight (Mw) of the SmGH3, AtGH3, and OsGH3 proteins were determined using the Compute pI/Mw tool on the ExPASy server (Wilkins et al., 1999).

## 2.2 Multiple sequence alignment and phylogenetic analyses

Using the Gblocks\_0.91b program (Castresana, 2000), we initially identified the conserved block of SmGH3, AtGH3, and OsGH3 proteins. Subsequently, a multiple sequence alignment of the conserved SmGH3, AtGH3, and OsGH3 proteins was performed using the DNAMAN program (Lynnon Corporation, San Ramon, CA, USA). Additionally, to determine sequence identities, pairwise comparisons were conducted using the MegAlign package of the DNAStar program with the SmGH3, AtGH3, and OsGH3 amino acid sequences. Furthermore, to investigate the evolutionary relationships among SmGH3, AtGH3, and OsGH3 genes, as well as to identify the orthologs and paralogs among these genes in thses three species, an unrooted tree was generated using Bayesian inference implemented in MrBayes (Huelsenbeck and Ronquist, 2001; Hall, 2005) based on the SmGH3, AtGH3, and OsGH3 amino acid sequences. The substitution model employed for the construction of the phylogenetic tree was JTT + I + G, which was selected using the PhyloSuite v1.2.1 program (Zhang et al., 2019). The phylogenetic tree was represented with the help of Treeview1.61 software (Zhai et al., 2002).

## 2.3 Gene structure analysis and motif detection

The gene structure of SmGH3, AtGH3, and OsGH3 was analyzed using the Gene Structure Display Server software (Guo et al., 2007), based on their respective coding sequences and corresponding gene sequences. The conserved motifs were identified in SmGH3, AtGH3, and OsGH3 proteins using the online MEME tool with the following parameters: the e-values less than 2 x  $10^{-30}$ , and any number of repetitions of a motif (Bailey et al., 2006; Zhang et al., 2015).

# 2.4 Cis-regulatory elements in the promoter regions analysis

To investigate the regulatory information of gene expression, we conducted a comprehensive analysis of *cis*-regulatory elements across the promoter regions of the *SmGH3*, *AtGH3*, and *OsGH3* genes. We extracted the 2.0 kb upstream sequence of the start codon (ATG) for each of these genes from their respective genomic scaffolds. Subsequently, we utilized the online platform of PlantCARE database (Lescot et al., 2002) to predict the *cis*-regulatory elements present in these promoter regions. Finally, we employed visualization tools available in TBtools (Chen et al., 2020) to generate detailed distribution maps of these *cis*-regulatory elements across each promoter region.

#### 2.5 Ka and Ks calculation

To detect whether Darwinian positive selection participated in promoting gene divergence following duplication, we identified the paralogs of SmGH3, AtGH3, and OsGH3 genes based on the phylogenetic tree. Then, we employed the PAL2NAL program (Suyama et al., 2006) to estimate the nonsynonymous (Ka) and synonymous (Ks) substitution rates, as well as the Ka/Ks ratio (nonsynonymous/synonymous substitution rate) for each paralogous gene pair. Generally, a Ka/Ks ratio of 1, greater than 1, and less than 1 indicates neutral evolution, positive selection, and negative or purifying selection, respectively (Wang et al., 2005). To further analyze selection pressures across gene regions, we calculated Ka/Ks ratios using a sliding window of 20 amino acids (Fares, 2004). Consistently, in regions where all paralogous genes showed evidence of neutral evolution, positive selection, or purifying selection, the Ka/Ks ratios consistently reflected these patterns, with ratios of 1, greater than 1, and less than 1, respectively (Fares, 2004; Wang et al., 2019).

## 2.6 Detection of positive selection

To preliminarily investigate whether the *GH3* gene family of *A. thaliana*, *S. miltiorrhiza*, and *O. sativa* exhibited evidence of positive selection (Yang et al., 2000), we examined the hypothesis of positive selection among the *GH3* genes in these species using the codeml program (Yang et al., 2000) in PAML (Phylogenetic Analysis by Maximum Likelihood) v4.9a (Nielsen and Yang, 1998; Yang, 2000, 2007) with site models and branch-site models.

In the site models, six codon substitution models M0 (one ratio), M3 (discrete), M1a (neutral), M2a (selection), M7 (beta), and M8 (beta +  $\omega$ ) were applied to identify codons subjected to positive selection and to detect the positively selected sites (Li et al., 2015; Wang et al., 2019). The codeml program was used to calculate the Ka/Ks ratio and to detect the variation in the  $\omega$  parameter among sites by performing likelihood ratio tests (LRTs) between the following site model comparisons: M0 vs. M3, M1a vs. M2a, and M7 vs. M8. The detailed information on codon substitution models can refer to the previous studies (Li et al., 2015; Wang et al., 2017, 2019). Branch-site models hypothesize the different evolutionary rates to vary among different sites and branches simultaneously (Yang, 2007). We applied the improved branch-site model to compare the ratio of Ka/Ks substitution rates between branches, and to detect the positive selection amino acid sites of SmGH3, AtGH3, and OsGH3 genes (Zhang et al., 2005). Consistent with previous methods (Li et al., 2015; Wang et al., 2017), in the branchsite model, all the branches were categorized into foreground and background groups. When the foreground branches were examined for positive selection, the other branches on the tree were used as the background. For each branch, the ratio of Ka/Ks substitution rates was calculated with the Null Model ( $\omega = 1$ ) and Alternative Model ( $\omega > 1$ ) (Li et al., 2015; Wang et al., 2017). The methods to identify the positive selection sits and estimate the Posterior probabilities (Qks) followed the previously described (Li et al., 2015; Wang et al., 2019).

## 2.7 Estimation of functional divergence

To investigate the functional divergence between subgroup genes of SmGH3, AtGH3, and OsGH3, we utilized the Diverge 3.0 software (Gu et al., 2013) to estimate significant changes in site-specific shifts based on maximum likelihood procedures. Then, we calculated the coefficients of Type-I and Type-II functional divergences ( $\theta_{\rm I}$  and  $\theta_{\rm II}$ ) between two clusters, following the previously described methods (Gu, 2006; Li et al., 2015; Wang et al., 2017, 2019). In brief,  $\theta_{\rm I} > 0$ indicates site-specific alerted selective constraints, while  $\theta_{II} > 0$ demonstrates a radical shift in amino acid physiochemical property happened following gene duplication or speciation, respectively (Gu, 1999; Li et al., 2015; Wang et al., 2019). Detailed interpretations of  $\theta_{\rm I}$ and  $\theta_{\rm II}$ , can be found in previous studies (Gu, 1999; Li et al., 2015; Wang et al., 2019). The neighbor-joining tree used for functional divergence analysis was reconstructed with the amino acid sequences of SmGH3, AtGH3, and OsGH3 under the MEGA 6.0 software (Tamura et al., 2013).

We also employed the Posterior probabilities (Qks) to identify amino acid sites associated with functional divergence. Generally, the larger Qk stands for the higher possibility that the evolutionary rate or the radical change in the amino acid property of a site that was different between the two groups (Gu, 2006; Li et al., 2015; Wang et al., 2019). Additionally, the Qk cutoff for identifying residues related to  $\theta_{\rm I}$  and  $\theta_{\rm II}$  between gene groups was determined following previously described methods (Gu, 2006; Li et al., 2015; Wang et al., 2019).

# 2.8 Expression analysis of AtGH3, OsGH3 and SmGH3 genes

For preliminary analysis of the expression patterns of AtGH3 and OsGH3 genes, we employed their CDS sequences as query sequences to identify EST sequences corresponding to these genes from the GenBank EST database (https://www.ncbi.nlm.nih.gov/ genbank/dbest/) (Boguski et al., 1993) using the blastn suite with default parameters. The identified EST sequences were considered to correspond to the GH3 genes if they met the following criteria: longer than 160 bp, with a threshold of less than  $10^{-10}$ , and a hit rate above 95% (Yang et al., 2008). Finally, the identified EST sequences were classified according to their tissue origin based on GENEVESTIGATOR (Zimmermann et al., 2004). Meanwhile, we analyzed the tissue-specific expression patterns of SmGH3 genes based on the RPKM (Reads Per Kilobase per Million) values of S. miltiorrhiza RNA-seq data from roots, stems, leaves, and flowers tissues (SRP051524, SRP051564, SRP028388) (Zhang et al., 2015), using the Mev program (Saeed et al., 2003).

## 3 Results

## 3.1 Sequence feature of GH3 genes in A. thaliana, S. miltiorrhiza, and O. sativa

With the 19 AtGH3 and OsGH3 amino acid sequences and the basic characteristics of GH3 protein, we carefully surveyed the S. miltiorrhiza genome, eight members of SmGH3 genes were identified (Supplementary Table 1). For the AtGH3, OsGH3, and SmGH3 genes, the lengths ranged from 2025 bp (AT1G48660) to 4064 bp (AT4G03400), 1561 bp (Os11g0528700) to 8610 bp (Os07g0671500), and 1996 bp (SMil\_00018075) to 4103 bp (SMil\_00006699), respectively (Supplementary Table 1). The corresponding protein lengths varied from 525 aa (AT1G48670) to 672 aa (AT5G13360), 441 aa (Os07g0576500) to 629 aa (Os05g0500900), and 406 aa (SMil\_00017300) to 624 aa (SMil\_00003673), respectively (Supplementary Table 1). Furthermore, the molecular weights of the AtGH3, OsGH3, and SmGH3 proteins ranged from 64.12 kDa (AT1G48660) to 75.87 kDa (AT5G13360), 67.37 kDa (Os01g0785400) to 69.02 kDa (Os06g0499500), and 45.82 kDa (SMil\_00017300) to 69.24 kDa (SMil\_00003673), respectively (Supplementary Table 1). Additionally, the theoretical isoelectric points (pI) of the proteins were observed to range from 4.91 (AT5G13320) to 6.08 (AT5G13360 and AT2G47750), 5.03 (Os11g0528700) to 6.87 (Os05g0143800), and 5.57 (SMil\_00016018) to 7.68 (SMil\_00006699), respectively (Supplementary Table 1).

### 3.2 Multiple sequence alignment analysis

Multiple sequence alignment showed that mostly members of SmGH3, AtGH3, and OsGH3 proteins contain two mainly motifs of nucleotide ATP/AMP binding motif 1 and hormone-binding motif 2 (Chang et al., 1997; Singh et al., 2014; Yu et al., 2018) (Supplementary Figure 1). Pairwise analyses of the SmGH3, AtGH3, and OsGH3 amino acid sequences showed that the overall similarity level ranged from as low as 25.2% between AT5G13360 and SMil\_00017300 to a notably high similarity of 92.2% between AT4G27260 and AT5G54510 (Supplementary Table 2). High homology levels suggest they may carry out essentially similar functions, whereas low homology levels may indicate their distinct evolutionary origins and functional diversification (Kumar et al., 2012).

## 3.3 Phylogenetic relationship analysis

Based on sequence homology, the GH3 proteins from these species were distinctly categorized into three major groups (I, II and III), which correlated with their functions and sequence similarities (Figure 1). High bootstrap values for all the subgroups indicated that the genes in each subgroup might share a similar origin, which advices that the same clusters could have the same function

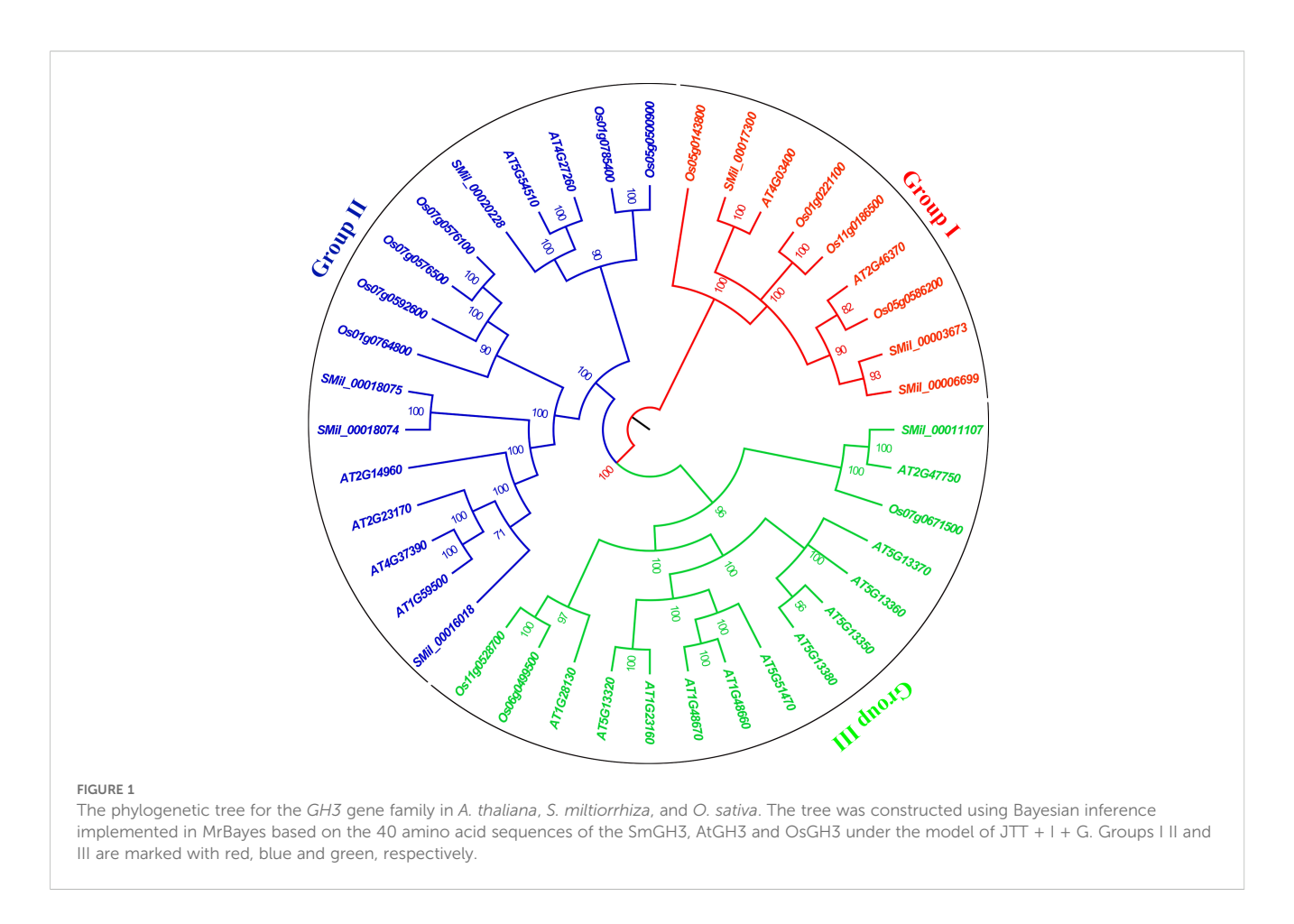
(Staswick et al., 2002, 2005). Group I comprises nine members, with three from S. miltiorrhiza, two from A. thaliana and four from O. sativa. Group II contains four SmGH3, six AtGH3, and six OsGH3 genes. Group III includes one SmGH3 gene, 11 AtGH3 genes, and three OsGH3 genes (Figure 1). Additionally, paralogous gene pairs within the SmGH3 gene family were identified, including SMil\_00018074 and SMil\_00018075 in Group II, and SMil\_00003673 and SMil\_00006699 in Group I (Figure 1). Within the AtGH3 gene family, five paralogous gene pairs were discovered, including AT1G48670 and AT1G48660; AT1G23160 and AT5G13320; AT5G13350 and AT5G13380 in Group III; AT1G59500 and AT4G37390; as well as AT5G54510 and AT4G27260 in Group II. Furthermore, in the OsGH3 gene family, four paralogous gene pairs were found: Os06g0499500 and Os11g0528700 in Group III (Figure 1), Os07g0576500 and Os07g0576100; Os01g0785400 and Os05g0500900 in Group II; and Os01g0221100 and Os11g0186500 belong to Group I (Figure 1).

## 3.4 Gene structure and motif analysis

Gene structure analysis revealed that the number of exons in *SmGH3*, *AtGH3*, and *OsGH3* genes ranged from one to six, and averaging three to four exons across the three species (Figure 2). Additionally, the number of introns varied from zero to five. Notably, a single intronless gene (*Os07g0576500*) was identified (Figure 2). Furthermore, the correlation between gene structure and phylogenetic tree analysis reveals that genes within the same group exhibit similar structural patterns, suggesting that genes in the same subgroup may share analogous functions (Figure 2).

With the online MEME suite, 22 conserved motifs within the amino acid sequences of AtGH3, OsGH3, and SmGH3 were identified. The normal expression sequences and diagram of these 22 motifs are listed in Supplementary Table 3 and 4, respectively. The results revealed that the frequencies of these motifs ranged from 7 to 40 (Supplementary Table 3). Additionally, the number of amino acids comprising each GH3 motif varied from 8 to 50, and the number of motifs present in each GH3 protein ranged from 11 to 19 (Supplementary Table 3). Moreover, among the motifs, motifs 2, 3, 4, 6, 8, 9, and 16 were commonly found in AtGH3, OsGH3, and SmGH3 proteins (Figure 3, Supplementary Table 4).

Furthermore, the integration of phylogenetic tree analysis with motif composition revealed that GH3 proteins within the same subgroup exhibited highly conserved motif arrangements and compositions (Figure 3), suggesting that genes within the same subgroup likely share analogous functional roles. Whereas, motifs 7, 10 and 12 were uniquely present in both Group I and Group II. Motif 19 was specifically found in Group I and Group III, while motifs 17 and 22 were exclusively present in Group III. Notably, motif 19 in Group I was uniquely identified in *A. thaliana*, and motif 14 in Group III was exclusively detected in *O. sativa* (Figure 3, Supplementary Table 4). These results suggest that group-specific sequence motifs are present in different groups, potentially contributing to functional divergence among these groups.

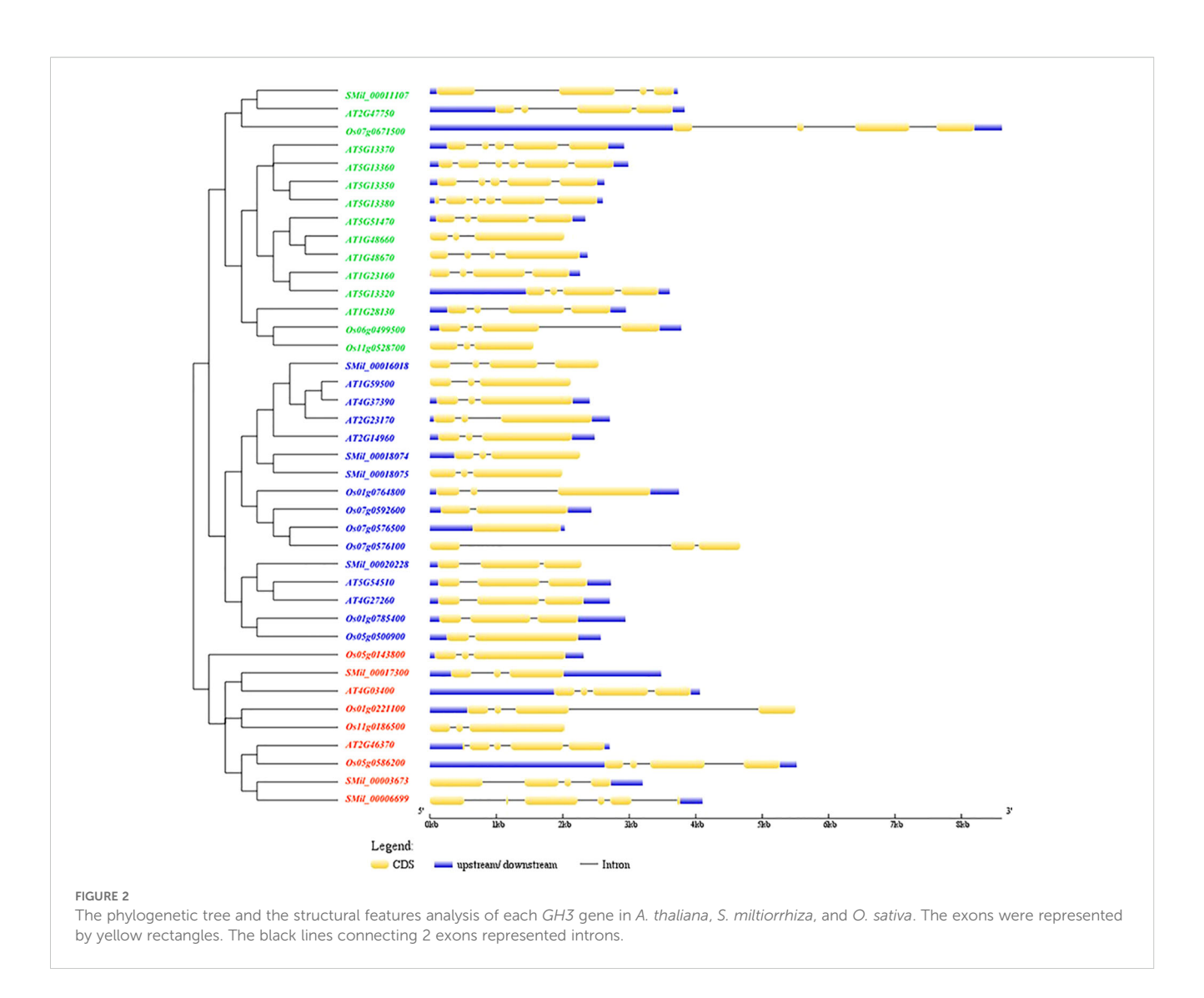


# 3.5 Cis-regulatory elements of promoter analysis in AtGH3, OsGH3 and SmGH3

The analysis of cis-regulatory elements within the promoter sequences revealed that they are enriched with plant hormone response elements. These include abscisic acid-responsive elements (ABREs), which are implicated in ABA signaling; CGTCA- and TGACG-motifs, which are involved in MeJA responsiveness; and TCA-elements specifically associated with SA signaling (Figure 4, Supplementary Table 5). Specifically, nearly all AtGH3, OsGH3, and SmGH3 gene promoters contain cis-regulatory elements implicated in MeJA-responsiveness (Figure 4, Supplementary Table 5). 20 GH3 gene promoters were found to harbor cis-regulatory elements associated with GA responsiveness, while 24 promoters contained elements linked to ABA responsiveness (Figure 4, Supplementary Table 5). Additionally, 15 GH3 gene promoters were associated with SA responsiveness, and 11 promoters contained auxin-responsive regulatory elements (Figure 4, Supplementary Table 5). These findings highlight the significant role of GH3 genes in plant hormone regulation. Furthermore, 14 GH3 gene promoters were found to contain cisregulatory elements associated with low-temperature responsiveness (LRT), while 10 promoters were identified to harbor MYB binding sites (MBS) linked to drought-inducibility (Figure 4, Supplementary Table 5). Notably, one GH3 gene promoter was found to contain a wound-responsive element (WUN-motif) (Figure 4, Supplementary Table 5). In light of these findings, it appears that the expression of the *GH3* gene is closely linked to various plant stress responses.

## 3.6 Driving forces for genetic divergence

To investigate the forces driving genetic divergence, we calculated the ratio of Ka/Ks with the coding sequences of paralogous pairs within the AtGH3, OsGH3, and SmGH3 genes. Our results showed that the Ka/Ks ratios were less than 1 for five AtGH3, four OsGH3, and two SmGH3 paralogous pairs, indicating that negative selection has acted on these genes (Supplementary Table 6). Meanwhile, we also calculated the Ka/Ks ratios for all the paralogous genes using a sliding window of 20 amino acids. Our results revealed that the Ka/Ks ratio was consistently less than 1 in most regions, with only a small fraction of regions showing a Ka/Ks ratio greater than 1 (Figure 5). Notably, two specific paralogous pairs, AT5g13350 and AT5g13380, as well as SMil\_00018074 and SMil\_00018075, exhibited a majority of their analyzed regions with Ka/Ks > 1 (Figure 5). Nevertheless, the overall Ka/Ks ratio for these genes remained below 1 (Supplementary Table 6). These findings further suggest that GH3 genes are divergent under the purifying pressure in A. thaliana, S. miltiorrhiza, and O. sativa.



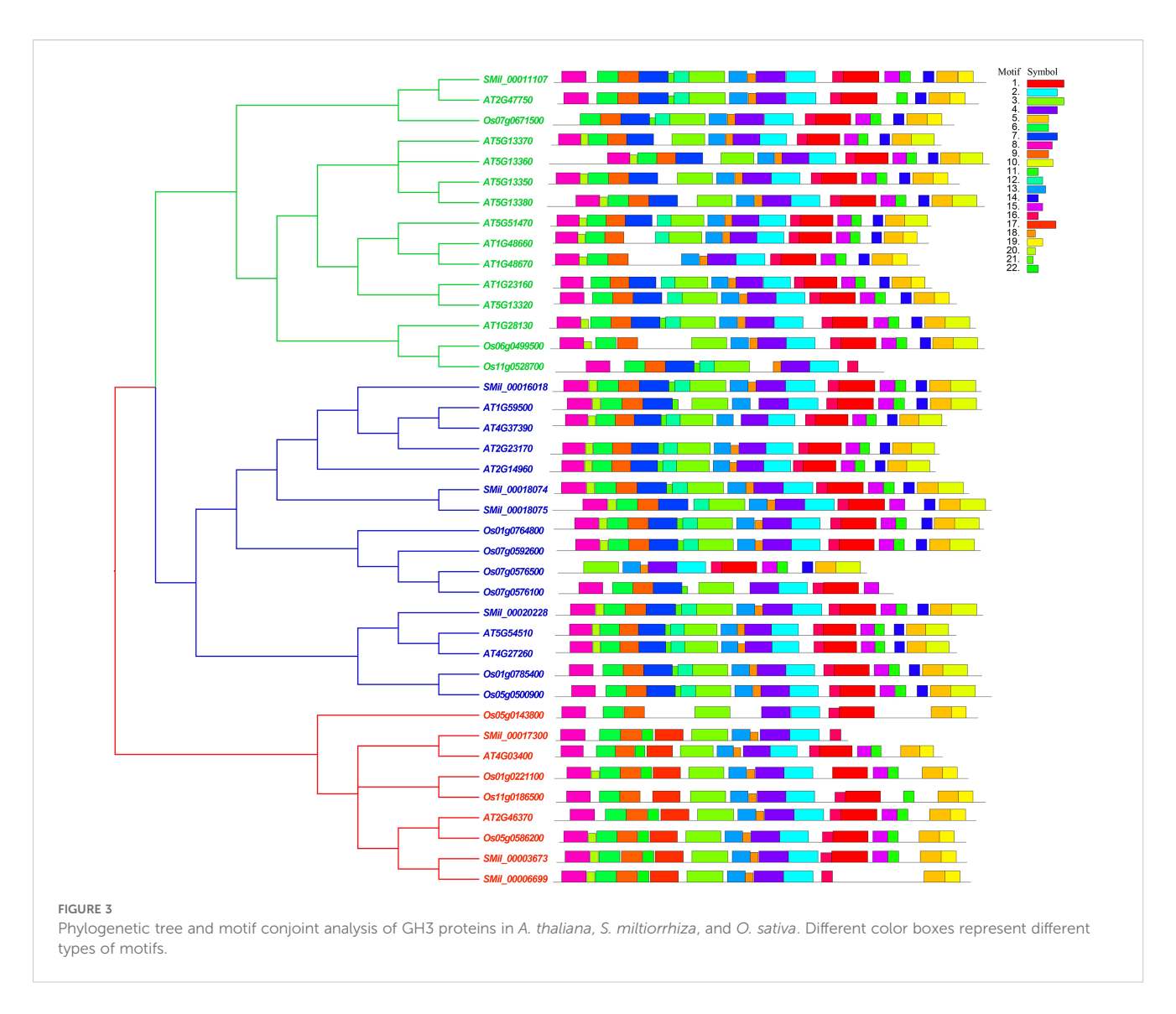
# 3.7 Positive selection on AtGH3, OsGH3 and SmGH3 genes

To preliminarily investigate the evolutionary mechanism of *GH3* gene family in *Arabidopsis*, *S. miltiorrhiza* and *O. sativa*, we assessed the hypothesis of positive selection of *AtGH3*, *OsGH3* and *SmGH3* genes using the PAML package (Yang et al., 2000; Yang, 2007).

In the site models, following the analysis method described in the previous study (Li et al., 2015; Wang et al., 2017, 2019), we compared the M0 vs. M3 to test how Ka/Ks ratios differed among codon positions. Under the M0 model, the log-likelihood value was  $\iota = -54531.985321$ , with a value of  $\omega = 0.13572$ . In the meantime, the M3 model yielded a log-likelihood value of  $\iota = -53113.4944310$ , with three  $\omega$  estimates ( $\omega_0 = 0.01691$ ,  $\omega_1 = 0.10134$ , and  $\omega_2 = 0.30575$ ). These results suggest that relaxed purifying selection is the predominant evolutionary force acting on the *GH3* gene family in *A. thaliana*, *S. miltiorrhiza* and *O. sativa* (Table 1). Furthermore, the twice log likelihood difference ( $2\Delta \ln L$ ) between M3 and M0 was calculated as 2836.98178 (Table 1), which was strongly statistically significant (p < 0.01) and suggested that M3 was better than M0.

Therefore, the results indicated that different sites bear different selection pressures and also revealed fluctuations in the overall level of selective constraints (Li et al., 2015; Wang et al., 2017, 2019). Next, the M2a vs. M1a and M8 vs. M7 were compared to test whether positive selection promoted divergence between genes (Li et al., 2015). The log-likelihood values for M1a and M2a were t= -54101.460731 and t= -54101.460957, respectively. Similarly, under models M7 and M8, the log-likelihood values were t= -53553.845867 and t= -53550.001494, respectively (Table 1). The 2 $\Delta$ lnL values for M2a vs. M1a and M8 vs. M7 were 0 and 7.39, respectively. Thus, in both comparisons, there was no statistical significance, and no site was detected under positive selection at the level of 95% (Table 1). All parameter estimates are presented in Table 1.

In branch-site models, we compared the Null and Alternative models to test the positive sites under positive selection in particular lineage groups. The results showed that the two models differed significantly (p < 0.01) when each lineage group was designated as the foreground branch. This suggests that the *GH3* lineage groups from *A. thaliana*, *S. miltiorrhiza*, and *O. sativa* exhibit distinct evolutionary rates (Table 2). Additionally, when the foreground



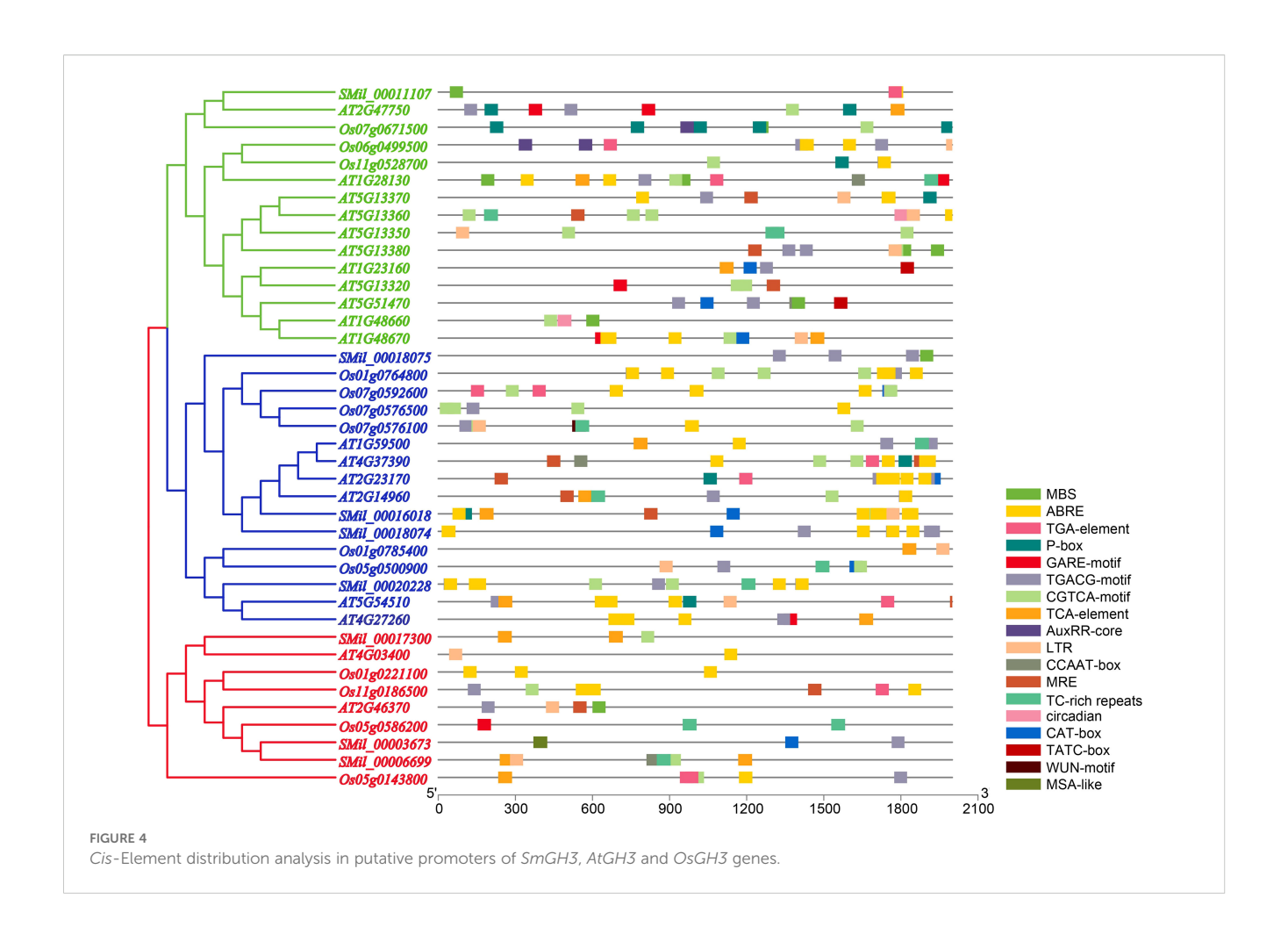
branch was assigned to group I, a total of 570 positively selected sites were found, with a 2 $\Delta$ lnL value of 38.546436 (p < 0.01) between Null and Alternative models. When the foreground branch was set to group II, 13 positively selected sites were identified, yielding a 2 $\Delta$ lnL value of 12.33403 (p < 0.01). Similarly, when the foreground branch was assigned to group III, 18 positively selected sites were detected, with a 2 $\Delta$ lnL value of 15.767194 (p < 0.01). These results indicate that all three lineage groups were under positive selection (p < 0.01). However, no site was positively selected at a level of 95% (Table 2). Furthermore, the remarkably higher number of positively selected sites in group I suggests that this group may be undergoing strong positive Darwinian selection compared to the other two groups. All parameter estimates are presented in Table 2.

# 3.8 Functional divergence analysis of SmGH3, AtGH3 and OsGH3 proteins

Based on the neighbor-joining tree, the *GH3* gene family in *A. thaliana*, *S. miltiorrhiza* and *O. sativa* were also divided into three

primary clusters (Supplementary Figure 2). Using the DIVERGE program, we evaluated the rates of evolutionary shift and the properties of altered amino acids following gene duplication (Gu, 1999; 2006).

The results revealed that the coefficients for the Type-I functional divergence ( $\theta_{\rm I}$ ) among Group I vs. Group II, Group I vs. Group III, and Group II vs. Group III were 0.561910, 0.440390 and 0.237761, respectively (Supplementary Table 7). Notably, all  $\theta_{\rm I}$ coefficients were greater than 0 across all group pairs. This suggested that some amino acid sites may have undergone significant site-specific changes between these group pairs, which bring about a subgroup-specific functional divergence during their evolution (Gu, 2006; Gu et al., 2013; Wang et al., 2017). Furthermore, the results also revealed that  $\theta_I$  values of Group I vs. Group II, Group I vs. Group III, and Group II vs. Group III were statistically significant (p < 0.01) (Supplementary Table 7). This observation is consistent with our phylogenetic analysis that functional divergence has occurred among members of different groups. In addition, the coefficients of Type-II functional divergence  $(\theta_{\rm II})$  for all three pairs were less than 0 ( $\theta_{\rm II}$  = -0.136874,  $\theta_{\rm II}$  =



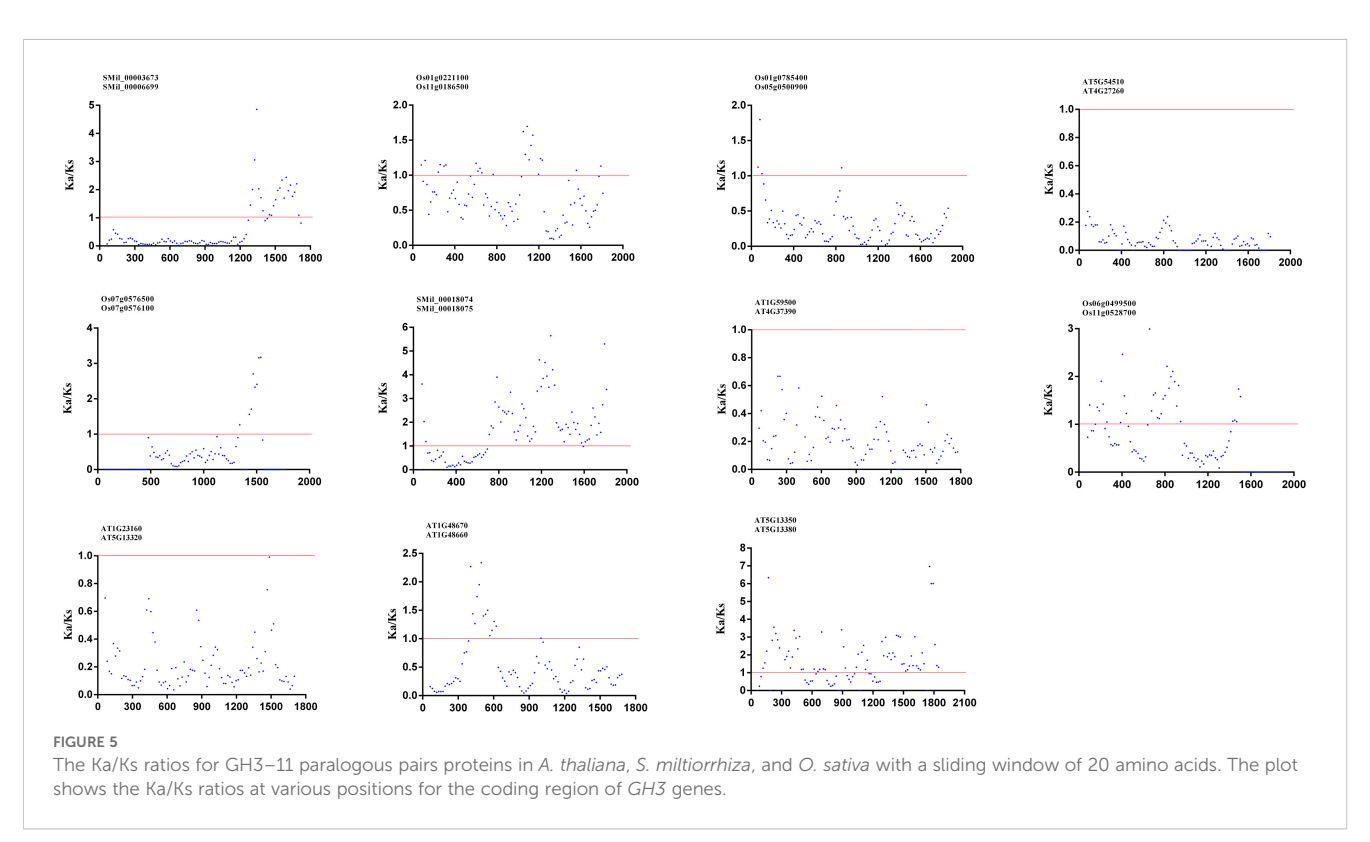


TABLE 1 Tests for positive selection among codons of SmGH3, AtGH3 and OsGH3 genes using site models.

Model	np	lnL	Estimates of parameter <sup>1</sup>		2∆lnL	Positive selection sites <sup>2</sup>
			Frequency	dN/dS		sites
M0 (one-ratio)	80	-54531.985321		0.13572		None
M3 (discrete)	84	-53113.494431	$p_0 = 0.18365$ $p_1 = 0.41779$ $p_2 = 0.39856$	$\omega_0 = 0.01691$ $\omega_1 = 0.10134$ $\omega_2 = 0.30575$	2836.98178(M3 vs. M0) **	Not allowed
M1a (nearly neutral)	81	-54101.460731	$p_0 = 0.82037$ $p_1 = 0.17963$	$\omega_0 = 0.13449$ $\omega_1 = 1.00000$		None
M2a (positive selection)	83	-54101.460957	$p_0 = 0.82037$ $p_1 = 0.17963$ $p_2 = 0.00000$	$\omega_0 = 0.13449$ $\omega_1 = 1.00000$ $\omega_2 = 318.98328$	0 (M2a vs. M1a)	Not allowed
M7 (beta)	81	-53553.845867	p = 0.87388 q = 3.76068			None
M8 (beta & ω)	83	-53550.001494	$p_0 = 0.97816$ $p = 0.90568$ $q = 4.17138$ $p_1 = 0.02184$	ω = 1.90498	7.392934 (M8 vs. M7) *	584 A

p < 0.05 and p < 0.01 (p < 0.01).

-0.637158 and  $\theta_{\rm II}$  = -0.283415), and not statistically significant among the three group pairs (p = 0.2514, p = 0.02275 and p = 0.08691, respectively) (Supplementary Table 8). Those results suggest that most amino acids of SmGH3, AtGH3, and OsGH3 proteins have not undergone significant changes in their physical and chemical properties (Li et al., 2015; Wang et al., 2017, 2019).

Additionally, the positive selection sites that influencing functional divergence between the groups was also tested using the Posterior probability (Qk). As previously described (Li et al., 2015; Wang et al., 2017, 2019), we established Qk > 0.8 and 1.0 as the threshold for identifying the Type-I and Type-II functional

divergence-related positive selection sites between groups, respectively. The analysis of Qks revealed that the distribution and the number of positive selection sites associated with functional divergence varied across group pairs. For Type-I functional divergence, when Qk > 0.8, all of the three clusters pairs contained positive selection sites (Figure 6). In contrast, for Type-II functional divergence, there was no group pair contained positive selection sites, when Qk > 1.0 (Figure 7). These results suggest that the identified positive selection sites probably play a crucial role in the functional divergence of SmGH3, AtGH3, and OsGH3 during their evolutionary process. The detailed distribution

TABLE 2 Selective pressure analyses of SmGH3, AtGH3 and OsGH3 genes using branch-site models.

Foreground branches	Branch-site model	lnL	2∆lnL	P Value	ω Values <sup>1</sup>	Positively selected sites <sup>2</sup>
Group I	Null	-54569.474808	38.546436	< 0.01	$\omega_0 = 0.13548 \ \omega_1 = 1.00000$ $\omega_2 = 1.00000$	570 Sites were detected
	Alternative	-54550.201590	38.340430		$\omega_0 = 0.13670 \ \omega_1 = 1.00000$ $\omega_2 = 999.00000$	
Group II	Null	-54589.735993	12 22402	< 0.01	$\omega_0 = 0.13470 \ \omega_1 = 1.00000$ $\omega_2 = 1.00000$	- 13 Sites were detected
	Alternative	-54583.568978	12.33403		$\omega_0 = 0.13475 \ \omega_1 = 1.00000$ $\omega_2 = 248.12040$	
Group III	Null	-54587.802687	15.767104	< 0.01	$\omega_0 = 0.13418 \ \omega_1 = 1.00000$ $\omega_2 = 1.00000$	- 18 Sites were detected
	Alternative	-54579.919090	15.767194		$\omega_0 = 0.13443 \ \omega_1 = 1.00000$ $\omega_2 = 21.24914$	

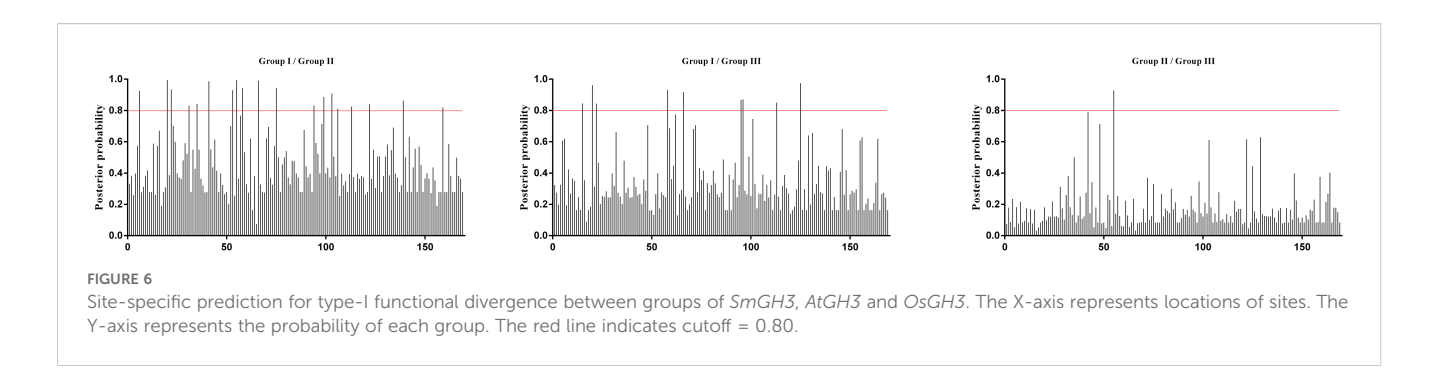
<sup>\*</sup>p < 0.05 and \*\*p < 0.01 ( $x^2$  test).

 $<sup>^{1}\</sup>omega$  was estimated under model M0, M3, M7, and M8; p and q are the parameters of the beta distribution.

<sup>&</sup>lt;sup>2</sup>The number of amino acid sites estimated to have undergone positive selection.

 $<sup>^{1}\</sup>omega$  was estimated under model Null and Alternative.

<sup>&</sup>lt;sup>2</sup>The number of amino acid sites estimated to have undergone positive selection.



patterns of positive selection sites influencing Type-I and Type-II functional divergence between groups are illustrated in Figure 6 and 7, Supplementary Tables 7 and 8.

# 3.9 The expression analysis of AtGH3, OsGH3 and SmGH3 genes

According to GENEVESTIGATOR, in A. thaliana and O. sativa, the ESTs primarily contain six tissue categories including Callus Cell, Suspension, Seedling, Inflorescence, Rosette, and Roots (Zimmermann et al., 2004). To preliminarily detect the tissuespecific expression of AtGH3 and OsGH3 genes, the CDS sequences of each GH3 gene were employed to search the A. thaliana and O. sativa ESTs databases with the blastn program. Because of the specially temporal and special expression pattern for genes, and the EST database may not contain the EST resource for certain genes (Yang et al., 2008), there were five AtGH3 genes and three OsGH3 genes that didn't find evidence of the expression (Supplementary Table 9, 10). In A. thaliana, most AtGH3 genes are predominantly expressed in tissues of Rosette, Root, and Inflorescence (Supplementary Table 9). Meanwhile, in O. sativa, most OsGH3 genes are primarily expressed in tissues of Seedling, Inflorescence, and Callus tissues (Supplementary Table 10).

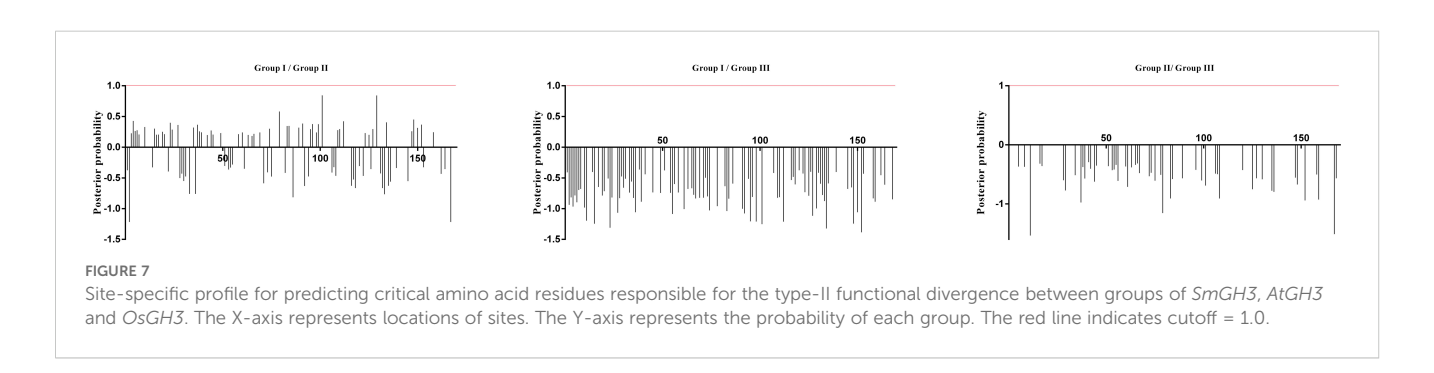
Based on the RPKM values derived from RNA-seq data for *S. miltiorrhiza* organs of root, stem, leaf and flower, we observed distinct expression patterns of these genes in different organs. Among these genes, *SMil\_00016018*, *SMil\_00018075*, and *SMil\_00018074* exhibited relatively low expression levels across all examined organs (Supplementary Figure 3, Supplementary Table 11). Specifically, *SMil\_00016018* and *SMil\_00018075* exhibited tissue-specific expression patterns, being detectable only

in the flowers and roots, while *SMil\_00018074* showed no expression in the leaves. In contrast, *SMil\_00006699* demonstrated relatively high expression levels across all four organs examined (Supplementary Figure 3, Supplementary Table 11). Additionally, *SMil\_00003673* and *SMil\_00011107* exhibited elevated expression levels in stems, whereas *SMil\_00017300* showed higher expression in flowers and leaves. Notably, *SMil\_00020228* demonstrated particularly high expression in roots (Supplementary Figure 3, Supplementary Table 11).

## 4 Discussion

The Gretchen Hagen 3 (GH3) proteins, a small multi-gene family within the acyl-adenylate/thioester-forming enzyme superfamily, play a critical role in regulating hormone homeostasis in plants (Baranwal et al., 2017; Kong et al., 2019). These proteins function by catalyzing the formation of amino acid conjugates, which in turn modulate various physiological processes (Kong et al., 2019). Consequently, the substrates and enzymatic products of GH3 proteins exert significant influence on plant development, growth regulation, and responses to environmental stress (Kong et al., 2019). As research progresses, an increasing number of GH3 gene families have been identified in diverse plant species, including mosses and angiosperms (Singh et al., 2014). Through in-depth studies of this gene family, the functions of GH3 genes in plant growth processes can be elucidated, while also allowing us to investigate the evolutionary relationships among different species.

The protein lengths of *GH3* family varied from 525 to 672 amino acids in *A. thaliana* (Staswick et al., 2002), 441 to 629 amino acids in *O. sativa* (Jain et al., 2006a), 547 to 651 amino acids in



maize (Feng et al., 2015), 578 to 613 amino acids in grape (Bottcher et al., 2011), 495 to 843 amino acids in tomato (Kumar et al., 2012), 571 to 614 amino acids in apple, 542 to 644 amino acids in cotton (Yu et al., 2018), and 588 to 640 amino acids in melon (Chen et al., 2023). This variation in protein lengths suggests that GH3 family members generally exhibit proteins longer than 400 amino acids. In this study, we identified eight GH3 genes in the genome of S. miltiorrhiza based on the sequence information of GH3 members from A. thaliana and O. sativa (Staswick et al., 2002; Jain et al., 2006b) and the reported protein lengths of GH3 genes. The GH3 family in S. miltiorrhiza is smaller than those in A. thaliana (19 members), O. sativa (13 members) and maize (13 members), but its size is comparable to that of grape (9 members). Furthermore, the parameters of SmGH3 proteins displayed high similarity to those of GH3 family in A. thaliana, O. sativa, maize and grape, suggesting that different GH3 proteins may perform analogous functions under varying microenvironmental conditions (Feng et al., 2015). The relatively high amino acid identity of SmGH3 genes (Supplementary Figure 1) also further indicates that these genes likely originated from a common ancestral sequence (Feng et al., 2015).

Gene duplications play a crucial role in gene family expansion, and Darwinian positive selection drives the expansion of gene families following duplication (Lynch and Conery, 2000). Phylogenetic analyses are essential for identifying putative paralogs, which are critical for detecting gene duplication events within gene families (Yang et al., 2008). Based on the phylogenetic tree, five pairs of paralogous genes were identified in A. thaliana, four pairs in O. sativa, and two pairs in S. miltiorrhiza (Figure 1). The findings revealed that a majority of AtGH3, OsGH3, and SmGH3 genes are organized as paralogous pairs (53% for A. thaliana, 62% for O. sativa, and 50% for S. miltiorrhiza). This indicates that over half of the GH3 genes in these species underwent duplication events, suggesting that AtGH3, OsGH3 and SmGH3 genes may have experienced gene family expansion following duplication during evolution (Wang et al., 2019). Additionally, tow sister pair genes (SMil\_00017300/AT4G03400 and SMil\_00011107/AT2G47750) within the GH3 gene family between S. miltiorrhiza and A. thaliana were identified as ortholog genes with a high bootstrap value of 100%. No sister gene pairs could be identified as orthologous between S. miltiorrhiza and O. sativa within the GH3 gene family (Figure 1). Notably, the phylogenetic relationship between S. miltiorrhiza and A. thaliana is significantly closer than that between S. miltiorrhiza and O. sativa. Our findings suggest that the functions of SmGH3 genes may share similarities with GH3 genes in A. thaliana.

Cis-regulatory elements are essential for gene transcription and expression, playing a crucial role in regulating plant adaptability to diverse environmental conditions through various molecular mechanisms (Liu et al., 2016; Yao et al., 2023). By investigating the multitude of cis-regulatory elements in the promoter regions of AtGH3, OsGH3 and SmGH3 genes, we could gain preliminary insights into the diverse functions of GH3 genes in plants growth and development. In the present study, we found that cis-regulatory elements associated with plant hormone response were significantly

represented among the promoter regions of *AtGH3*, *OsGH3* and *SmGH3* genes (Figure 4, Supplementary Table 5). This finding suggested that the expression of *GH3* genes may be modulated through multiple plant hormone pathways. Additionally, the promoters of *AtGH3*, *OsGH3* and *SmGH3* genes were found to contain numerous stress-related regulatory elements, which was consistent with previous study that *GH3* genes are widely involved in disease resistance and biotic and abiotic stress responses (Jain and Khurana, 2009; Feng et al., 2015; Ai et al., 2023).

Our analysis of the Ka/Ks ratios for AtGH3, OsGH3 and SmGH3 paralogs revealed that all these ratios were less than 1 (Supplementary Table 6). Moreover, the sliding window analysis indicated that regions exhibiting Ka/Ks ratios greater than 1 across all paralogous genes were relatively rare (Figure 5). These results collectively suggest that GH3 genes in these species have likely been subject to negative selection, which play a dominant role in driving force the gene divergence. This finding is consistent with previous studies on wheat, Oryza species, and Rosaceae species (Kong et al., 2019; Jiang et al., 2020; Guo et al., 2025). Additionally, site models analysis demonstrated that different sites within the GH3 gene family are subject to varying selection pressures, and purifying selection has also been a dominant force in the evolution of the GH3 gene family in S. miltiorrhiza, A. thaliana and O. sativa. Furthermore, although most positive sites were identified during the branch-site model analysis, none achieved statistical significance (p < 0.05) (Table 2). These results indicate that despite exposure to positive Darwinian selection across all subgroups and sites, the GH3 gene family in A. thaliana, S. miltiorrhiza and O. sativa primarily underwent neutral evolution and negative selection. All those findings collectively provided further evidence to support our driving force analysis for the gene divergence.

In accordance with prior research, GH3 genes are classified into three distinct groups (I, II, and III), which are characterized by significant functional divergence among their members (Staswick et al., 2002, 2005; Okrent et al., 2009). Our analysis of adaptive evolution revealed that group I has experienced strong positive Darwinian selection relative to the other two groups, likely reflecting the potential functional roles of its constituent genes. Group I GH3 proteins are primarily characterized as JA- or SAamido synthetases, catalyzing the conversion of these hormones into their respective conjugated forms, such as JA-Ile and SAamides (Staswick et al., 2002). JA and JA-Ile function as critical hormonal signaling molecules, regulating plant secondary metabolism, growth, defense, and development (Pieterse et al., 1998; Chehab et al., 2012; Pingping et al., 2017). Notably, most GH3 genes are up-regulated by JA treatment (Feng et al., 2015). SA, a key phytohormone, plays a pivotal role in plant immunity defense (Gao et al., 2014) and serves as a major stress-related hormone involved in plant growth and development under abiotic stresses (Xiong et al., 2002). Consequently, the execution of these defensive functions may necessitate that GH3 genes experience stronger positive selective pressure to enhance their adaptive potential to environmental challenges.

Motif analysis demonstrated that GH3 proteins from different subgroups exhibit distinct motif compositions and arrangements

(Supplementary Table 4), which are indicative of specific amino acid residue changes that may contribute to functional divergence among these subgroups. Using the DIVERGE program, we conducted an in-depth analysis of the molecular mechanisms underlying this functional divergence. The results further demonstrated that specific amino acid residues underwent site-specific changes that contributed to functional divergence among *GH3* ubgroup genes in *S. miltiorrhiza*, *A. thaliana* and *O. sativa* throughout the course of their evolution.

The tissue-specific expression of *AtGH3*, *OsGH3* and *SmGH3* genes exhibit differential expression across various tissues, potentially indicating distinct functional roles in different tissues. Similar to other species (Jain and Khurana, 2009; Feng et al., 2015), *SmGH3* exhibited tissue-specific expression patterns in *S. miltiorrhiza*. Based on the RPKM values, most *SmGH3* displayed relatively lower expression levels in the leaves compared to other organs (Supplementary Figure 3, Supplementary Table 11). These findings are consistent with previous studies on tissue-specific expression of *GH3* genes in other species, such as maize (Feng et al., 2015), tomato (Kumar et al., 2012), and apple (Yuan et al., 2013). Notably, most *SmGH3* genes were relatively highly expressed in stems, suggesting their potential roles in stem growth and development rather than in leaves.

Tissue-specific expression analysis revealed that SMil\_00020228 exhibits particularly high expression in roots (Supplementary Figure 3, Supplementary Table 11). Phylogenetic analysis demonstrated that SMil\_00020228 clusters with SiGH3.15 (Supplementary Figure 4), which regulates lateral root development through modulation of auxin homeostasis in tomato (Ai et al., 2023). Moreover, the pharmacologically active components of S. miltiorrhiza are primarily localized in its roots, and the dried roots of S. miltiorrhiza have been used widely to treat various cardiovascular diseases (Wang et al., 2007; Kai et al., 2011). We propose that SMil\_00020228 likely plays a significant role not only in root development but also in the accumulation of pharmacologically active compounds in S. miltiorrhiza. Additionally, AtGH3.9 (AT2G4775) was involved in cross talk between auxin and JA signal transduction pathways by conjugating amino acids to both methyl jasmonate and auxin, respectively (Khan and Stone, 2007; Feng et al., 2015). Similarly, in maize, ZmGH3.9 is strongly induced by JA treatment in leaves (Feng et al., 2015). In S. miltiorrhiza, the closest homolog to both AtGH3.9 and ZmGH3.9 is SMil\_00011107 (Figure 1, Supplementary Figure 4). Based on this homology, we hypothesize that SMil\_00011107 functions as a jasmonate-responsive gene, playing a crucial role in regulating the JA signaling pathway within S. miltiorrhiza. Furthermore, phylogenetic tree reveals that SMil\_00016018 clusters with SiGH3.4, a gene that is strongly activated in the Arbuscular Mycorrhizal fungal-colonized roots, as demonstrated by previous studies in tomato (Liao et al., 2015; Chen et al., 2021). Moreover, as shown our tissue-specific expression analysis, SMil\_00016018 exhibited relatively low expression levels across all examined organs. Interestingly, this expression pattern closely resembles that of SiGH3.4 in tomato (Liao et al., 2015). Based on these observations, we hypothesize that SMil\_00016018

may play a role analogous to SiGH3.4 in mycorrhizal symbiosis within S. miltiorrhiza.

JAR1 (Jasmonic acid resistant 1) a key enzyme in jasmonate biosynthesis, is central to activating JA signaling and regulating defense and stress responses in plants (Suza and Staswick, 2008; Mosblech et al., 2011). Recently, GH3.10 has emerged as another critical catalyst for JA-Ile synthesis, complementing the role of JAR1 (Delfin et al., 2022; Ni et al., 2025). Evolutionary analysis reveals that SMil\_00017300 clusters closely with AtGH3.10 (AT4G03400) and SiGH3.10 (Kumar et al., 2012) (Figure 1, Supplementary Figure 4). Based on these phylogenetic relationships, we hypothesize that SMil\_00017300 may play a similar functional role to JAR1 in regulating JA signaling and defense mechanisms in S. miltiorrhiza. Indeed, SMil\_00017300 catalyzes the conversion of JA to JA-Ile, a biosynthetic step analogous to JAR1 activity (Shimizu et al., 2013; Delfin et al., 2022; Ni et al., 2025). JA-Ile signaling leads to the degradation of Jasmonate ZIM-domain (JAZ) proteins (Fonseca et al., 2009; Kramell et al., 2009), thereby releasing transcription factors such as MYB and MYC for activation (Ding et al., 2017; Shasha et al., 2018). Notably, both phenolic acids and tanshinones—signature bioactive compounds in S. miltiorrhiza—are regulated by JA signaling (Xiao et al., 2009; Wang et al., 2016) and their biosynthesis is directly influenced by MYB and MYC transcription factors (Zhang et al., 2014). Consequently, SmGH3 genes exert regulatory control over endogenous hormone homeostasis in S. miltiorrhiza, which in turn modulates downstream signaling cascades, and subsequently influencing the biosynthesis of pharmacologically active components.

## 5 Conclusion

In this study, we characterized the GH3 gene family in S. miltiorrhiza and performed a comparative analysis of the GH3 gene family across three plant species: S. miltiorrhiza, A. thaliana and O. sativa. Our analysis integrated multiple approaches, including phylogenetic tree construction, GH3 domain characterization, gene structure and conserved motif identification, cis-regulatory elements examination, selective constraint analysis, functional divergence analysis, and expression profiling. Phylogenetic analysis revealed that the 40 AtGH3, OsGH3 and SmGH3 genes could be clustered into three distinct subgroups. Genetic divergence analyses indicated that the GH3 genes from S. miltiorrhiza, A. thaliana, and O. sativa have been subjected to purifying selection pressure. Positive selection and functional divergence analyses further demonstrated that these GH3 genes have undergone purifying selective pressure and have diverged in their functional roles. Based on an integrated analysis of phylogenetic evolution and tissue-specific expression patterns, our findings suggest that certain members of the SmGH3 gene family are involved in responding to the jasmonates signaling pathway, thereby playing critical roles in the biosynthesis and accumulation of pharmacologically active compounds, as well as in secondary metabolism in S. miltiorrhiza. Collectively, these results provide a comprehensive understanding of the GH3 gene family, offering valuable insights for future functional studies of *GH3* genes in plants.

## Data availability statement

The datasets presented in this study can be found in online repositories. The names of the repository/repositories and accession number(s) can be found in the article/supplementary material.

## **Author contributions**

BW: Writing – review & editing, Writing – original draft, Visualization, Methodology, Validation. ML: Writing – review & editing, Methodology, Investigation, Data curation. JC: Methodology, Funding acquisition, Formal Analysis, Resources, Writing – original draft, Software. LC: Data curation, Visualization, Writing – original draft.

## **Funding**

The author(s) declare financial support was received for the research and/or publication of this article. The authors acknowledge financial support from Doctoral Research Initiation Foundation of Henan Normal University (Project no: 20250205), Jiangxi province project Education Fund (Project no: GJJ170434), National Natural Science Foundation of China (Project no: 21968001).

## Acknowledgments

The authors are grateful to all data analysis participants for very useful comments and data processing assistance.

### Conflict of interest

The authors declare that the research was conducted in the absence of any commercial or financial relationships that could be construed as a potential conflict of interest.

#### References

Adams, M. D., Kerlavage, A. R., Fleischmann, R. D., Fuldner, R. A., Bult, C. J., Lee, N. H., et al. (1995). Initial assessment of human gene diversity and expression patterns based upon 83 million nucleotides of cDNA sequence. *Nature* 377, 3.

Ai, G., Huang, R., Zhang, D., Li, M., Li, G., Li, W., et al. (2023). *SlGH3.15*, a member of the *GH3* gene family, regulates lateral root development and gravitropism response by modulating auxin homeostasis in tomato. *Plant Sci.* 330, 111638. doi: 10.1016/iplantsci.2033.111638.

Altschul, S. F., Madden, T. L., Schäffer, A. A., Zhang, J., Zhang, Z., Miller, W., et al. (1997). Gapped BLAST and PSI-BLAST: a new generation of protein database search programs. *Nucleic Acids Res.* 25, 3389–3402. doi: 10.1093/nar/25.17.3389

Bailey, T. L., Williams, N., Misleh, C., and Li, W. W. (2006). MEME: discovering and analyzing DNA and protein sequence motifs. *Nucleic Acids Res.* 34, 369–373. doi: 10.1093/nar/gkl198

Baranwal, V. K., Negi, N., and Khurana, P. (2017). Auxin response factor genes repertoire in Mulberry: identification, and structural, functional and evolutionary analyses. *Genes* 8, 202. doi: 10.3390/genes8090202

#### Generative AI statement

The author(s) declare that no Generative AI was used in the creation of this manuscript.

Any alternative text (alt text) provided alongside figures in this article has been generated by Frontiers with the support of artificial intelligence and reasonable efforts have been made to ensure accuracy, including review by the authors wherever possible. If you identify any issues, please contact us.

### Publisher's note

All claims expressed in this article are solely those of the authors and do not necessarily represent those of their affiliated organizations, or those of the publisher, the editors and the reviewers. Any product that may be evaluated in this article, or claim that may be made by its manufacturer, is not guaranteed or endorsed by the publisher.

## Supplementary material

The Supplementary Material for this article can be found online at: https://www.frontiersin.org/articles/10.3389/fpls.2025.1644853/full#supplementary-material

#### SUPPLEMENTARY FIGURE 1

The multiple sequence alignments of the SmGH3, AtGH3 and OsGH3 protein conserved domain, including the nucleotide (ATP/AMP) and hormone-binding motif 1 and hormone-binding motif 2.

#### SUPPLEMENTARY FIGURE 2

The neighbor-joining phylogenetic tree was reconstructed with GH3 amino acid sequences of *A. thaliana*, *S. miltiorrhiza*, and *O. sativa* using MEGA 6.0.

#### SUPPLEMENTARY FIGURE 3

Heatmaps representing the expression profiles of  $\mathit{SmGH3}$ , genes in the Flower, Leaf, Root and Stem.

### SUPPLEMENTARY FIGURE 4

The phylogenetic tree for the GH3 gene family in maize (Zea mays), tomato (Solanum lycopersicum), and S. miltiorrhiza.

Boguski, M. S., Lowe, T. M. J., and Tolstoshev, C. M. (1993). dbEST — database for "expressed sequence tags. *Nat. Genet.* 4, 332-333. doi: 10.1038/ng0893-332

Bottcher, C., Boss, P. K., and Davies, C. (2011). Acyl substrate preferences of an IAA-amido synthetase account for variations in grape (*Vitis vinifera* L.) berry ripening caused by different auxinic compounds indicating the importance of auxin conjugation in plant development. *J. Exp. Bot.* 62, 4267–4280. doi: 10.1093/jxb/err134

Castresana, J. (2000). Selection of conserved blocks from multiple alignments for their use in phylogenetic analysis. *Mol. Biol. Evol.* 17, 540–552. doi: 10.1093/oxfordjournals.molbev.a026334

Chang, K. H., Xiang, H., and Dunaway-Mariano, D. (1997). Acyl-adenylate motif of the acyl-adenylate/thioester-forming enzyme superfamily: A site-directed. *Biochemistry* 36, 15650–15659. doi: 10.1021/bi971262p

Chehab, E. W., Yao, C., Henderson, Z., Kim, S., and Braam, J. (2012). *Arabidopsis* touch-induced morphogenesis is jasmonate mediated and protects against Pests. *Curr. Biol.* 22, 701–706. doi: 10.1016/j.cub.2012.02.061

- Chen, X., Chen, J., Liao, D., Ye, H., Li, C., Luo, Z., et al. (2021). Auxin-mediated regulation of arbuscular mycorrhizal symbiosis: A role of *SIGH3.4* in tomato. *Plant Cell Environ.* 45, 955–968. doi: 10.1111/pce.14210
- Chen, C., Chen, H., Zhang, Y., Thomas, H. R., and Xia, R. (2020). TBtools: an integrative toolkit developed for Interactive analyses of big biological data. *Mol. Plant* 13, 1194-1202. doi: 10.1016/j.molp.2020.06.009
- Chen, Y., Hao, X., and Cao, J. (2014). Small auxin upregulated RNA (SAUR) gene family in maize: Identification, evolution, and its phylogenetic comparison with Arabidopsis, rice, and sorghum. *J. Integr. Plant Biol.* 56, 133–150. doi: 10.1111/jipb.12127
- Chen, S., Zhong, K., Li, Y., Bai, C., Xue, Z., and Wu, Y. (2023). Evolutionary analysis of the Melon (*Cucumis melo L.*) *GH3* gene family and identification of *GH3* genes related to fruit growth and development. *Plants* 12, 1382. doi: 10.3390/plants12061382
- Cui, B., Liang, Z., Liu, Y., Liu, F., and Zhu, J. (2012). Effects of ABA and its biosynthetic inhibitor fluridone on accumulation of penolic acids and activity of PAL and TAT in hairy root of *Salvia miltiorrhiza*. *China J. Chin. Materia Med.* 37, 754–759. doi: 10.1111/j.1365-313X.1991.00051.x
- Delfin, J. C., Kanno, Y., Seo, M., Kitaoka, N., Matsuura, H., Tohge, T., et al. (2022). *AtGH3.10* is another jasmonic acid-amido synthetase in *Arabidopsis thaliana*. *Plant J.* 110, 1082–1096. doi: 10.1111/tpj.15724
- Ding, K., Pei, T., Bai, Z., Jia, Y., Ma, P., and Liang, Z. (2017). SmMYB36, a novel R2R3-MYB transcription factor, enhances tanshinone accumulation and decreases phenolic acid content in Salvia miltiorrhiza hairy roots. Sci. Rep. 7, 5104. doi: 10.1038/s41598-017-04909-w
- Fares, M. A. (2004). SWAPSC: sliding window analysis procedure to detect selective constraints. *Bioinformatics* 20, 2867–2868. doi: 10.1002/(SICI)1520-6378(199810) 23:53.0.CO:2-S
- Feng, S., Yue, R., Yang, S. T. Y., Zhang, L., Xu, M., Wang, H., et al. (2015). Genome-wide identification, expression analysis of auxin-responsive *GH3* family genes in maize (*Zea mays* L.) under abiotic stresses. *J. Integr. Plant Biol.* 57, 783–795. doi: 10.1111/jipb.12327
- Fonseca, S., Chico, J. M., and Solano, R. (2009). The jasmonate pathway: the ligand, the receptor and the core signalling module. *Curr. Opin. Plant Biol.* 12, 539–547. doi: 10.1016/j.pbi.2009.07.013
- Fu, J., Yu, H., Li, X., Xiao, J., and Wang, S. (2011). Rice GH3 gene family: regulators of growth and development. Plant Signal Behav. 6, 570–574. doi: 10.4161/psb.6.4.14947
- Gao, F., Dai, R., Pike, S. M., Qiu, W., and Gassmann, W. (2014). Functions of *EDS1*-like and *PAD4* genes in grapevine defenses against powdery mildew. *Plant Mol. Biol.* 86, 381–393. doi: 10.1007/s11103-014-0235-4
- Garcia-Hernandez, M., Berardini, T. Z., Chen, G., Crist, D., Doyle, A., Huala, E., et al. (2002). TAIR: a resource for integrated *Arabidopsis* data. *Funct. Integr. Genomics* 2, 239–253. doi: 10.1007/s10142-002-0077-z
- Ge, Q., Zhang, Y., Hua, W. P., Wu, Y. C., Jin, X. X., Song, S. H., et al. (2015). Combination of transcriptomic and metabolomic analyses reveals a JAZ repressor in the jasmonate signaling pathway of *Salvia miltiorrhiza*. *Sci. Rep.* 5, 14048. doi: 10.1038/srep14048
- Geng, Z. H., Huang, L., Song, M. B., and Song, Y. M. (2015). Cardiovascular effects in vitro of a polysaccharide from Salvia miltiorrhiza. Carbohydr Polym 121, 241–247. doi: 10.1016/j.carbpol.2014.12.038
- Gu, X. (1999). Statistical methods for testing functional divergence after gene duplication. *Mol. Biol. Evol.* 16, 1664. doi: 10.1007/s12020-008-9067-9
- Gu, X. (2006). A simple statistical method for estimating type-II (cluster-specific) functional divergence of protein sequences. *Mol. Biol. Evol.* 23, 1937–1945. doi: 10.1093/molbev/msl056
- Gu, X., Zou, Y., Su, Z., Huang, W., Zhou, Z., Arendsee, Z., et al. (2013). An update of DIVERGE software for functional divergence analysis of protein family. *Mol. Biol. Evol.* 30, 1713–1719. doi: 10.1093/molbev/mst069
- Guo, L., Lu, S., Gou, H., Ren, J., Yang, J., Zeng, B., et al. (2025). Evolution analysis of *GH3* gene family in five Rosaceae species and *FaGH3.17*, *FaGH3.18* improve drought tolerance in transgenic *Arabidopsis*. *BMC Plant Biol*. 25. doi: 10.1186/s12870-025-06689.2
- Guo, A. Y., Zhu, Q. H., Chen, X., and Luo, J. C. (2007). GSDS: a gene structure display server. Hereditas 29, 1023–1026. doi: 10.1360/yc-007-1023
- Hagen, G., and Guilfoyle, K. T. (1984). Auxin-regulated gene expression in intact soybean hypocotyl and excised hypocotyl sections. *Planta* 162, 147–153. doi: 10.1007/BF00410211
- Hall, T. A. (1999). BioEdit: A user-friendly biological sequence alignment editor and analysis program for windows 95/98/NT. *Nucle Acids Symposium Ser.* 41, 95–98. doi: 10.1021/bk-1999-0734.ch008
- Hall, B. G. (2005). Comparison of the accuracies of several phylogenetic methods using protein and DNA sequences. *Mol. Biol. Evol.* 22, 792–802. doi: 10.1093/molbev/msi066
- Huang, B., Qi, Y., Huang, X., and Yang, P. (2023). Genome-wide identification and co-expression network analysis of Aux/IAA gene family in *Salvia miltiorrhiza*. *PeerJ* 11, e15212. doi: 10.7717/peerj.15212
- Huelsenbeck, J. P., and Ronquist, F. (2001). MRBAYES: Bayesian inference of phylogenetic trees. *Bioinformatics* 17, 754–755. doi: 10.1093/bioinformatics/17.8.754

- Jain, M., Kaur, N., Tyagi, A. K., and Khurana, J. P. (2006a). The auxin-responsive *GH3* gene family in rice (*Oryza sativa*). Funct. Integr. Genomics 6, 36–46. doi: 10.1007/s10142-005-0142-5
- Jain, M., and Khurana, J. P. (2009). Transcript profiling reveals diverse roles of auxin-responsive genes during reproductive development and abiotic stress in rice. *FEBS J.* 276, 3148–3162. doi: 10.1111/J.1742-4658.2009.07033.X
- Jain, M., Tyagi, A. K., and Khurana, J. P. (2006b). Genome-wide analysis, evolutionary expansion, and expression of early auxin-responsive SAUR gene family in rice (*Oryza sativa*). *Genomics* 88, 360–371. doi: 10.1016/j.ygeno.2006.04.008
- Jiang, W., Yin, J., Zhang, H., He, Y., Shuai, S., Chen, S., et al. (2020). Genome-wide identification, characterization analysis and expression profiling of auxin-responsive *GH3* family genes in wheat (*Triticum aestivum L.*). *Mol. Biol. Rep.* 47, 3885–3907. doi: 10.1007/s11033-020-05477-5
- Kai, G., Xu, H., Zhou, C., Liao, P., and Zhang, L. (2011). Metabolic engineering tanshinone biosynthetic pathway in *Salvia miltiorrhiza* hairy root cultures. *Metab. Eng.* 13, 319–327. doi: 10.1016/j.ymben.2011.02.003
- Khan, S., and Stone, J. (2007). *Arabidopsis thaliana GH3.9* in auxin and jasmonate cross talk. *Plant Signaling Behav.* 2, 483–485. doi: 10.4161/psb.2.6.4498
- Kong, W., Zhong, H., Deng, X., Gautam, M., Gong, Z., Zhang, Y., et al. (2019). Evolutionary analysis of *GH3* genes in six *Oryza* species/subspecies and their expression under salinity stress in *Oryza sativa* ssp. japonica. *Plants (Basel)* 8. doi: 10.3390/plants8020030
- Kramell, R., Miersch, O., Wasternack, C., Solano, R., Fonseca, S., Chini, A., et al. (2009). (+)-7-iso-Jasmonoyl-L-isoleucine is the endogenous bioactive jasmonate. *Nat. Chem. Biol.* 5, 344–350. doi: 10.1038/nchembio.161
- Kumar, R., Agarwal, P., Tyagi, A. K., and Sharma, A. K. (2012). Genome-wide investigation and expression analysis suggest diverse roles of auxin-responsive *GH3* genes during development and response to different stimuli in tomato (*Solanum lycopersicum*). *Mol. Genet. Genomics* 287, 221–235. doi: 10.1007/s00438-011-0672-6
- Lescot, M., Déhais, P., Thijs, G., Marchal, K., Moreau, Y., Van De Peer, Y., et al. (2002). PlantCARE, a database of plant cis-acting regulatory elements and a portal to tools for in silico analysis of promoter sequences. *Nucleic Acids Res.* 30, 325–327. doi: 10.1093/nar/30.1.325
- Li, C., Li, D., Shao, F., and Lu, S. (2015). Molecular cloning and expression analysis of WRKY transcription factor genes in Salvia miltiorrhiza. BMC Genomics 16, 200. doi: 10.1186/s12864-015-1411-x
- Liao, D., Chen, X., Chen, A., Wang, H., Liu, J., Liu, J., et al. (2015). The characterization of six auxin-induced tomato *GH3* genes uncovers a member, *SIGH3.4*, strongly responsive to arbuscular mycorrhizal symbiosis. *Plant Cell Physiol.* 56, 674–687. doi: 10.1093/pcp/pcu212
- Liu, L., Xu, W., Hu, X., Liu, H., and Lin, Y. (2016). W-box and G-box elements play important roles in early senescence of rice flag leaf. Sci. Rep. 6. doi: 10.1038/srep20881
- Lynch, M., and Conery, J. S. (2000). The evolutionary fate and consequences of duplicate genes. *Science* 290, 1151. doi: 10.1126/science.290.5494.1151
- Ma, Y., Yuan, L., Wu, B., Li, X., Chen, S., and Lu, S. (2012). Genome-wide identification and characterization of novel genes involved in terpenoid biosynthesis in *Salvia miltiorrhiza*. *J. Exp. Bot.* 63, 2809–2823. doi: 10.1093/jxb/err466
- Mosblech, A., Thurow, C., Gatz, C., Feussner, I., and Heilmann, I. (2011). Jasmonic acid perception by COI1 involves inositol polyphosphates in *Arabidopsis thaliana*. *Plant J.* 65, 949–957. doi: 10.1111/j.1365-313X.2011.04480.x
- Ni, B., Klein, M., Hossbach, B., Feussner, K., Hornung, E., Herrfurth, C., et al. (2025). *Arabidopsis GH3.10* conjugates jasmonates. *Plant Biol.* 27, 476–491. doi: 10.1111/plb.70001
- Nielsen, R., and Yang, Z. (1998). Likelihood models for detecting positively selected amino acid sites and applications to the HIV-1 envelope gene. *Genetics* 148, 929–936. doi: 10.1046/j.1365-2443.1998.00179.x
- Nobuta, K., Okrent, R. A., Stoutemyer, M., Rodibaugh, N., Kempema, L., Wildermuth, M. C., et al. (2007). The *GH3* acyl adenylase family member PBS3 regulates salicylic acid-dependent defense responses in *Arabidopsis. Plant Physiol.* 144, 1144–1156. doi: 10.1104/pp.107.097691
- Ohlrogge, J., and Benning, C. (2000). Unraveling plant metabolism by EST analysis. *Curr. Opin. Plant Biol.* 3, 224–228. doi: 10.1016/S1369-5266(00)80069-2
- Okrent, R. A., Brooks, M. D., and Wildermuth, M. C. (2009). *Arabidopsis GH3.12* (*PBS3*) conjugates amino acids to 4-substituted benzoates and is inhibited by salicylate. *J. Biol. Chem.* 284, 9742-9754. doi: 10.1074/jbc.M806662200
- Okrent, R. A., and Wildermuth, M. C. (2011). Evolutionary history of the *GH3* family of acyl adenylases in rosids. *Plant Mol. Biol.* 76, 489–505. doi: 10.1007/s11103-011-9776-y
- Park, J. E., Seo, P. J., Lee, A. K., Jung, J. H., Kim, Y. S., and Park, C. M. (2007). An *Arabidopsis GH3* Gene, encoding an auxin-conjugating enzyme, mediates phytochrome b-regulated light signals in hypocotyl growth. *Plant Cell Physiol.* 48, 1236–1241. doi: 10.1093/pcp/pcm086
- Pieterse, C. M. J., Wees, S. C. M. V., Pelt, J., Knoester, M., Laan, R., Gerrits, H., et al. (1998). A novel signaling pathway controlling induced systemic resistance in *Arabidopsis. Plant Cell* 10, 1571–1580. doi: 10.2307/3870620
- Pingping, N., Xia, L., Shune, W., Jianhua, G., Hongwei, Z., and Dongdong, N. (2017). Induced systemic resistance against botrytis cinerea by bacillus cereus AR156 through a

- JA/ET- and NPR1-dependent signaling pathway and activates PAMP-Triggered immunity in *Arabidopsis*. Front. Plant Sci. 8. doi: 10.3389/fpls.2017.00238
- Saeed, A. I., Sharov, V., White, J., Li, J., Liang, W., Bhagabati, N., et al. (2003). TM4: a free, open-source system for microarray data management and analysis. *BioTechniques* 34, 374–378. doi: 10.1089/154065803762851360
- Sakai, H., Lee, S. S., Tanaka, T., Numa, H., Kim, J., Kawahara, Y., et al. (2013). Rice annotation project database (RAP-DB): an integrative and interactive database for rice genomics. *Plant Cell Physiol.* 54, e6. doi: 10.1093/pcp/pcs183
- Shasha, L., Yucui, W., Jing, K., Huaiqin, W., Tangzhi, D., Yaya, H., et al. (2018). SmMYB111 is a key factor to phenolic acid biosynthesis and interacts with both SmTTG1 and SmbHLH51 in Salvia miltiorrhiza. J. Agric. Food Chem. 66, 8069–8078. doi: 10.1021/acs.jafc.8b02548
- Shimizu, T., Miyamoto, K., Miyamoto, K., Minami, E., Nishizawa, Y., Iino, M., et al. (2013). OsJARI contributes mainly to biosynthesis of the stress-induced jasmonoylisoleucine involved in defense responses in rice. Biosci. Biotechnol. Biochem. 77, 1556–1564. doi: 10.1271/bbb.130272
- Shin-Ichiro, T., Nobuyoshi, M., and Akira, N. (2002). Expression of the *AtGH3a* Gene, an *Arabidopsis* homologue of the Soybean *GH3* Gene, is regulated by phytochrome B. *Plant Cell Physiol.* 43, 281–289. doi: 10.1093/pcp/pcf033
- Singh, V. K., Jain, M., and Garg, R. (2014). Genome-wide analysis and expression profiling suggest diverse roles of *GH3* genes during development and abiotic stress responses in legumes. *Front. Plant Sci.* 5. doi: 10.3389/fpls.2014.00789
- Song, J. Y., Luo, H. M., Chun-Fang, L. I., Chao, S., Jiang, X. U., and Chen, S. L. (2013). Salvia miltiorrhiza as medicinal model plant. Acta Pharm. Sin. 48, 1099.
- Staswick, P. E., Serban, B., Rowe, M., Tiryaki, I., Maldonado, M. T., Maldonado, M. C., et al. (2005). Characterization of an *Arabidopsis* enzyme family that conjugates amino acids to indole-3-acetic acid. *Plant Cell* 17, 616–627. doi: 10.1105/tpc.104.026690
- Staswick, P. E., Tiryaki, I., and Rowe, M. L. (2002). Jasmonate response locus JAR1 and several related *Arabidopsis* genes encode enzymes of the firefly luciferase superfamily that show activity on Jasmonic, salicylic, and indole-3-acetic acids in an assay for adenylation. *Plant Cell* 14, 1405–1415. doi: 10.1105/tpc.000885
- Suyama, M., Torrents, D., and Bork, P. (2006). PAL2NAL: robust conversion of protein sequence alignments into the corresponding codon alignments. *Nucleic Acids Res.* 34, W609–W612. doi: 10.1093/nar/gkl315
- Suza, W. P., and Staswick, P. E. (2008). The role of JAR1 in Jasmonoyl-L: -isoleucine production during *Arabidopsis* wound response. *Planta* 227, 1221–1232. doi: 10.1007/s00425-008-0694-4
- Takase, T., Nakazawa, M., Ishikawa, A., Kawashima, M., and Matsui, M. (2010). ydk1-D, an auxin-responsive *GH3* mutant that is involved in hypocotyl and root elongation. *Plant J.* 37, 471–483. doi: 10.1046/j.1365-313X.2003.01973.x
- Tamura, K., Stecher, G., Peterson, D., Filipski, A., and Kumar, S. (2013). MEGA6: molecular evolutionary genetics analysis version 6.0. *Mol. Biol. Evol.* 30, 2725–2729. doi: 10.1093/molbev/mst197
- Terol, J., Domingo, C., and Talón, M. (2006). The *GH3* family in plants: Genome wide analysis in rice and evolutionary history based on EST analysis. *Gene* 371, 279–290. doi: 10.1016/j.gene.2005.12.014
- Wang, S. K., Bai, Y. H., Shen, C. J., Wu, Y. R., Zhang, S. N., Jiang, D. A., et al. (2010). Auxin-related gene families in abiotic stress response in *Sorghum bicolor. Funct. Integr. Genomics* 10, 533–546. doi: 10.1007/s10142-010-0174-3
- Wang, B., Li, M., Yuan, Y., and Liu, S. (2019). Genome-wide comprehensive analysis of the SABATH Gene Family in *Arabidopsis* and rice. *Evolutionary Bioinf.* 15, 117693431986086. doi: 10.1177/1176934319860864
- Wang, X., Morris-Natschke, S. L., and Lee, K. H. (2007). New developments in the chemistry and biology of the bioactive constituents of Tanshen. *Med. Res. Rev.* 27, 133–148. doi: 10.1002/med.20077
- Wang, B., Niu, J., Li, B., Huang, Y., Han, L., Liu, Y., et al. (2018). Molecular characterization and overexpression of *SmJMT* increases the production of phenolic acids in *Salvia miltiorrhiza*. *Int. J. Mol. Sci.* 19, 3788. doi: 10.3390/ijms19123788
- Wang, B., Wang, S., and Wang, Z. (2017). Genome-wide comprehensive analysis the molecular phylogenetic evaluation and tissue-specific expression of SABATH gene family in *Salvia miltiorrhiza*. *Genes* 8. doi: 10.3390/genes8120365
- Wang, C. H., Zheng, L. P., Tian, H., and Wang, J. W. (2016). Synergistic effects of ultraviolet-B and methyl jasmonate on tanshinone biosynthesis in *Salvia miltiorrhiza* hairy roots. *J. Photochem. Photobiol. B: Biol.* 159, 93–100. doi: 10.1016/j.jphotobiol.2016.01.012
- Wang, W., Zheng, H., Yang, S., Yu, H., Li, J., Jiang, H., et al. (2005). Origin and evolution of new exons in rodents. *Genome Res.* 15, 1258–1264. doi: 10.1101/gr.3929705

- Wilkins, M. R., Gasteiger, E., Bairoch, A., Sanchez, J. C., and Hochstrasser, D. F. (1999). Protein Identification and Analysis Tools in the ExPASy Server. *Methods Mol. Biol.* 112, 531-552. doi: 10.1385/1-59259-890-0:571
- Woodward, A. W., and Bartel, B. (2005). Auxin: regulation, action, and interaction. Ann. Bot. 95, 707–735. doi: 10.1093/aob/mci083
- Xiao, Y., Gao, S., Di, P., Chen, J., Chen, W., and Zhang, L. (2009). Methyl jasmonate dramatically enhances the accumulation of phenolic acids in *Salvia miltiorrhiza* hairy root cultures. *Physiol. Plant* 137, 1–9. doi: 10.1111/j.1399-3054.2009.01257.x
- Xiong, L., Schumaker, K. S., and Zhu, J.-K. (2002). Cell signaling during cold, drought, and salt stress. *Plant Cell* 14, S165–S183. doi: 10.1105/tpc.000596
- Xu, Z., Peters, R. J., Weirather, J., Luo, H., Liao, B., Zhang, X., et al. (2015). Full-length transcriptome sequences and splice variants obtained by a combination of sequencing platforms applied to different root tissues of *Salvia miltiorrhiza* and tanshinone biosynthesis. *Plant J.* 82, 951–961. doi: 10.1111/tpj.12865
- Xu, H., Song, J., Luo, H., Zhang, Y., Li, Q., Zhu, Y., et al. (2016). Analysis of the genome sequence of the medicinal plant *Salvia miltiorrhiza*. *Mol. Plant* 9, 949–952. doi: 10.1016/j.molp.2016.03.010
- Yang, Z. (2000). Maximum likelihood estimation on large phylogenies and analysis of adaptive evolution in human influenza virus A. *J. Mol. Evol.* 51, 423–432. doi: 10.1007/s002390010105
- Yang, Z. (2007). PAML 4: phylogenetic analysis by maximum likelihood. *Mol. Biol. Evol.* 24, 1586–1591. doi: 10.1093/molbev/msm088
- Yang, Z., Nielsen, R., Goldman, N., and Pedersen, A. M. (2000). Codon-substitution models for heterogeneous selection pressure at amino acid sites. *Genetics* 155, 431–449. doi: 10.1093/genetics/155.1.431
- Yang, Z., Wang, X., Gu, S., Hu, Z., Xu, H., and Xu, C. (2008). Comparative study of SBP-box gene family in *Arabidopsis* and rice. *Gene* 407, 1–11. doi: 10.1016/j.gene.2007.02.034
- Yao, P., Zhang, C., Qin, T., Liu, Y., Liu, Z., Xie, X., et al. (2023). Comprehensive analysis of *GH3* gene family in potato and functional characterization of *StGH3.3* under drought stress. *Int. J. Mol. Sci.* 24, 15122. doi: 10.3390/ijms242015122
- Yu, D., Qanmber, G., Lu, L., Wang, L., Li, J., Yang, Z., et al. (2018). Genome-wide analysis of cotton *GH3* subfamily II reveals functional divergence in fiber development, hormone response and plant architecture. *BMC Plant Biol.* 18. doi: 10.1186/s12870-018-1545-5
- Yuan, H., Zhao, K., Lei, H., Shen, X., and Li, T. (2013). Genome-wide analysis of the GH3 family in apple ( $Malus \times domestica$ ). BMC Genomics 14, 297–297. doi: 10.1186/1471-2164-14-297
- Zhai, Y., Tchieu, J., and XXXJr., S. M. (2002). A web-based Tree View (TV) program for the visualization of phylogenetic trees. *J. Mol. Microbiol. Biotechnol.* 4, 69–70. doi: 10.1038/sj.jim.7000176
- Zhang, D., Gao, F., Jakovlić, I., Zou, H., and Wang, G. T. (2019). PhyloSuite: An integrated and scalable desktop platform for streamlined molecular sequence data management and evolutionary phylogenetics studies. *Mol. Ecol. Resources* 20, 348-355. doi: 10.1111/1755-0998.13096
- Zhang, S. W., Li, C. H., Cao, J., Zhang, Y. C., Zhang, S. Q., Xia, Y. F., et al. (2009). Altered architecture and enhanced drought tolerance in rice via the down-regulation of indole-3-acetic acid by TLD1/OsGH3.13 activation. *Plant Physiol* 151, 1889-1901. doi: 10.1104/pp.109.146803
- Zhang, X., Luo, H., Xu, Z., Zhu, Y., Ji, A., Song, J., et al. (2015). Genome-wide characterisation and analysis of *bHLH* transcription factors related to tanshinone biosynthesis in *Salvia miltiorrhiza*. *Sci. Rep.* 5, 11244. doi: 10.1038/srep11244
- Zhang, J., Nielsen, R., and Yang, Z. (2005). Evaluation of an improved branch-site likelihood method for detecting positive selection at the molecular level. *Mol. Biol. Evol.* 22, 2472–2479. doi: 10.1093/molbev/msi237
- Zhang, Y., Yan, Y.-P., Wu, Y.-C., Hua, W.-P., Chen, C., Ge, Q., et al. (2014). Pathway engineering for phenolic acid accumulations in *Salvia miltiorrhiza* by combinational genetic manipulation. *Metab. Eng.* 21, 71–80. doi: 10.1016/j.ymben.2013.10.009
- Zhao, J.-L., Zhou, L.-G., and Wu, J.-Y. (2010). Effects of biotic and abiotic elicitors on cell growth and tanshinone accumulation in *Salvia miltiorrhiza* cell cultures. *Appl. Microbiol. Biotechnol.* 87, 137–144. doi: 10.1007/s00253-010-2443-4
- Zhou, L., Zuo, Z., and Chow, M. S. (2005). Danshen: an overview of its chemistry, pharmacology, pharmacokinetics, and clinical use. *J. Clin. Pharmacol.* 45, 1345–1359. doi: 10.1177/0091270005282630
- Zimmermann, P., Hirschhoffmann, M., Hennig, L., and Gruissem, W. (2004). GENEVESTIGATOR. *Arabidopsis* mcroarray database and analysis toolbox. *Plant Physiol.* 136, 2621. doi: 10.1104/pp.104.046367